Received: 25 January 2021 | Accepted: 6 April 2021

DOI: 10.1002/wcms.1539

ADVANCED REVIEW

WIREs COMPUTATIONAL MOLECULAR SCIENCE WILEY

Finite temperature quantum dynamics of complex systems: Integrating thermo-field theories and tensor-train methods

Raffaele Borrelli[1] | **Maxim F. Gelin**[2]

[1]DISAFA, University of Torino, Grugliasco, Italy

[2]School of Sciences, Hangzhou Dianzi University, Hangzhou, China

Correspondence
Raffaele Borrelli, DISAFA, University of Torino, Largo Paolo Braccini 2, I-10095 Grugliasco (TO), Italy.
Email: raffaele.borrelli@unito.it

Funding information
Horizon 2020 Framework Programme, Grant/Award Number: 826013; The University of Torino, Grant/Award Number: BORR-RILO-19-01

Edited by Peter R. Schreiner, Editor-in-Chief

Abstract

This review provides the fundamental theoretical tools for the development of a complete wave-function formalism for the study of time-evolution of chemico-physical systems at finite temperature. The methodology is based on the non-equilibrium thermo-field dynamics (NE-TFD) representation of quantum mechanics, which is alternative to the commonly used density matrix representation. TFD concepts are extended and integrated with the tensor-train (TT) numerical tools leading to a novel and powerful theoretical and computational framework for the study of complex quantum dynamical problems. In addition, NE-TFD techniques are extended to enable the study of dissipative open systems via a new formulation of the hierarchical equations of motion (HEOM) fully integrated with TT methodologies. We demonstrate that the combination of the TFD machinery with computational advantages of TTs results in a powerful theoretical and computational framework for scrutinizing dynamics of complex multidimensional electron-vibrational systems. We illustrate the validity and the computational advantages of the developed methodologies by applying them to the study of quantum coherence effects in the energy-transfer processes in antenna systems, to the analysis of fingerprints of vibrational modes in electron-transfer and charge-transfer processes in various model and realistic multidimensional molecular systems, as well as to simulation of other fundamental models of physical chemistry.

This article is categorized under:

Theoretical and Physical Chemistry > Reaction Dynamics and Kinetics
Theoretical and Physical Chemistry > Statistical Mechanics

KEYWORDS

HEOM, quantum dynamics, tensor-train, thermo-field dynamics, time-dependent variational principle

1 | INTRODUCTION

The accurate simulation of time-dependent molecular processes is a fundamental problem of modern theoretical chemistry.[1] In the last three decades, new progress in quantum dynamics theory associated with unprecedented development of numerical methodologies for the representation of multivariate functions[2,3] have boosted the application of time-dependent quantum theory to the study of a variety of phenomena including, among others, multidimensional time-resolved spectroscopy,[4–6] non-equilibrium transport properties of materials,[7,8] energy and electron transfer.[9–12]

The time-dependent Schrödinger equation is the cornerstone of the analysis of non-equilibrium properties of molecular systems, and its solution represents the main obstacle to the understanding of most chemico-physical problems. From a purely numerical point of view the key issue is that the amount of memory and the number of operations required to solve the time-dependent Schrödinger equation grow exponentially with the number of degrees of freedom (DoFs) N, that is, the dependence has the form p^N with $p > 1$. This problem, which is rooted in the fundamental laws of quantum mechanics, and in the mathematical structure of Hilbert spaces on the top of which it is built, cannot be circumvented. The only possible way for scientists to tackle quantum problems of large dimensionality is to exploit some inherent simplification or "good approximation" of the many–body interactions. Tensor network approximations of the wave function are certainly a most promising tool for such a purpose. Multiconfiguration time-dependent Hartree and its multilayer formulation[13–15] as well as the Numerical Density-Matrix Renormalization Group (NDMRG),[16] are special classes of tensor network based methods.

Both are based on a basis set representation of the molecular wave-function and are capable of handling a large variety of Hamiltonian operators. However, they become unhandy in high temperature cases, as they require statistical sampling of the initial conditions, which introduces both theoretical and computational problems.[17–20] To circumvent these problems a very effective formalism can be used, which enables the treatment of finite temperature effects embedded into a pure wave function description known as thermo-field dynamics (TFD).[21] Similarity with the finite temperature approach developed in NDMRG[16] will be described in Section 2.

TFD was introduced in the 1970s to provide a finite temperature representation of quantum mechanics within the wave-function formalism.[22] While it had a deep impact on many problems of theoretical physics,[23–26] it did not receive much attention in molecular quantum dynamics: the first applications were reported relatively recently[27,28] and their number increased slowly ever since.[29–33]

Since in TFD the total number of DoFs is double that of the original system, special attention has to be paid to the numerical solution of the resulting dynamical problem. The methodology must have favorable scaling properties with respect to the number of nuclear DoFs.

This review is focused on three fundamental topics. Firstly, in Section 2 we present a theoretical method for the simulation of time-dependent properties of electron-vibrational systems with many DoFs at finite temperature based on TFD. Secondly, in Section 3 we show how to take advantage of recently developed techniques based on tensor networks to solve the resulting dynamical problem.[34] In particular we demonstrate that the tensor train (TT) decomposition, also known as matrix product state (MPS) representation, can provide a robust and efficient numerical framework for the solution of the TFD Schrödinger Equation.[34–36] Applications of the new computational framework are presented and discussed in Section 4.

Finally, in Section 5 we show how to take advantage of the twin-space formalism, the mathematical structure at the basis of TFD, to derive a new set of Hierarchical Equations of Motion (HEOM) for the reduced density matrix completely equivalent to the original methodology proposed by Tanimura and Kubo[37] that represents one of the most advanced theories to study quantum properties of condensed phase systems. A novel TT approach to the solution of the new HEOMs is also developed, and applications to model chemico-physical processes are presented, clearly showing the validity and the high computational efficiency of the new methodology.

2 | NON-EQUILIBRIUM THERMO-FIELD DYNAMICS

2.1 | Double space formalism

Before introducing TFD we briefly sketch the fundamental mathematical structure of the so-called "twin-space" formulation of quantum statistical mechanics, also referred to as non-equilibrium thermo-field dynamics (NE-TFD).[38] In this formulation a double Hilbert space is defined, $\mathscr{L} = \left(\mathcal{H} \otimes \tilde{\mathcal{H}}\right)$, where, $\tilde{\mathcal{H}}$ is the Hilbert space of a fictitious dynamical

system identical to the original Hilbert space $\mathcal{H}$ of the real physical systems.[39–41] If $\{m\tilde{n}\rangle\}$ is an orthonormal basis of $\mathscr{L}$ then

$$\langle m\tilde{n}|m'\tilde{n}'\rangle = \delta_{mm'}\delta_{\tilde{n}\tilde{n}'} \quad \sum_{mn} |\, m\tilde{n}\rangle\langle m\tilde{n}\,| = 1.$$

Further, the identity vector $|I\rangle$ is defined as

$$|\, I\rangle = \sum_{m} |\, m\tilde{m}\rangle. \tag{1}$$

This special vector allows to define a mapping between the dual space of $\mathcal{H}$ (i.e., the bra space) and the tilde space, indeed we have

$$\langle m|I\rangle = |\tilde{m}\rangle \quad \langle\tilde{m}|I\rangle = |m\rangle. \tag{2}$$

Using these relations it is possible to associate a vector of the $\mathscr{L}$ space to each operator A acting in the space $\mathcal{H}$

$$|\, A\rangle = A\,|\, I\rangle. \tag{3}$$

Similarly, we can define a state vector $|\rho(t)\rangle = \rho(t)\,|\, I\rangle$, where $\rho(t)$ is the density matrix of the system. Accordingly, the expectation value of A is defined as the scalar product

$$\langle A(t)\rangle = \langle A|\rho(t)\rangle = \langle I|A\rho(t)|I\rangle \equiv \mathrm{tr}(A\rho(t)). \tag{4}$$

The meaning of the above notation can be easily understood using the closure relation

$$|\, A\rangle = A\,|\, I\rangle = \sum_{mn} |\, m\tilde{n}\rangle\langle m\tilde{n}|A|I\rangle = \sum_{mn}\langle m|A|n\rangle\,|\, m\tilde{n}\rangle = \sum_{mn} A_{mn}\,|\, m\tilde{n}\rangle$$

whence it is clear that the vector $|A\rangle$ is a linear combination of a basis of $\mathscr{L}$ with coefficients given by the matrix elements A_{mn}. Together with operators acting in the space $\mathcal{H}$ it is possible to define a set of operators acting in the space $\mathcal{H}$. In particular, following Suzuki,[39] two operators A and B are weakly equivalent if

$$A\,|\, I\rangle = B\,|\, I\rangle \tag{5}$$

and we write

$$A \simeq B. \tag{6}$$

For each Hermitian operator A acting in the space $\mathcal{H}$ it is possible to define a tilde operator $\tilde{A}$ that is weakly equivalent to A as

$$A\,|\, I\rangle = \tilde{A}^{\dagger}\,|\, I\rangle \rightarrow A \simeq \tilde{A}^{\dagger} \tag{7}$$

where the dag operator implies the Hermitian conjugation. Consequently, for Hermitian operators

$$A \simeq \tilde{A}. \tag{8}$$

The tilde operator can be obtained from the original operators by the so-called tilde conjugation rules[40]

$$(AB)^{\sim} = \tilde{A}\tilde{B} \quad (c_1A + c_2B)^{\sim} = c_1^*\tilde{A} + c_2^*\tilde{B} \tag{9}$$

and

$$(c_1|n\rangle + c_2|m\rangle)^{\sim} = c_1^*|\tilde{n}\rangle + c_2^*|\tilde{m}\rangle. \tag{10}$$

If A, B are two operators of the space $\mathcal{H}$ and $\hat{A} = A - \tilde{A}^{\dagger}$ then

$$\hat{A}B\,|\,I\rangle = \left(A - \tilde{A}^{\dagger}\right)B\,|\,I\rangle = \left(AB - B\tilde{A}^{\dagger}\right)|\,I\rangle = (AB - BA)\,|\,I\rangle = [A,B]\,|\,I\rangle \tag{11}$$

proving the fundamental property of the twin-space formalism

$$[A,B] \simeq \hat{A}B. \tag{12}$$

Finally, we notice that the identity vector $|I\rangle$ is invariant under any unitary transformation of the original Hilbert space basis set $|m\rangle$.[40]

Equation (12) allows to rewrite quantum statistical mechanics in a commutator-free way. Indeed, it is easy to demonstrate that the evolution of the vector $|\rho(t)\rangle$ is given by the equation ($\hbar = 1$)

$$\frac{\partial}{\partial t}|\,\rho(t)\rangle = -i\left(H - \tilde{H}\right)|\,\rho(t)\rangle = -i\hat{H}\,|\,\rho(t)\rangle \qquad |\,\rho(0)\rangle = |\,\rho_0\rangle \tag{13}$$

where $\tilde{H}$ is a Hamiltonian operator identical to the physical Hamiltonian H but acting in the *tilde* space $\tilde{\mathcal{H}}$. The superoperator $\hat{H} = H - \tilde{H}$ acts in the entire $\mathscr{L}$ space and is the Liouville operator rewritten as a superoperator in the $\mathscr{L}$ space. We refer the reader to the demonstration reported in the original articles by Schmutz[41] and by Suzuki.[39] When the initial condition of the system can be described by a Boltzmann distribution with a certain zero-order Hamiltonian operator H_0 we have

$$|\,\rho(0)\rangle = Z_0^{-1}e^{-\beta H_0}\,|\,I\rangle \tag{14}$$

where Z_0 is the partition function and $\beta = 1/k_BT$, k_B being Boltzmann's constant and T is the temperature. It is now worth comparing the above formulation with the more common double-space theory[42] for clarifying similarities and differences of the two approaches. In double-space theory the notation $|mn\rangle\rangle = |m\rangle\langle n|$ is often used to identify a state of a space that is the direct product of $\mathcal{H}$ and its dual.[42,43] Once we let the tilde space and the dual space coincide this approach and the twin formalism seem identical.[44] However, in standard double-space formulation what is often referred to as Liouville superoperator is a mere symbol for a commutator, $L = [H, \cdot]$, which induces a Lie algebra in the Liouville space. In the twin-formulation outlined above the introduction of the tilde space and of its operators allows to eliminate all the commutators, overcoming the difficulties inherent in their evaluation, and replace them with the action of an operator in a Hilbert space. From a mathematical point of view the double vector $|I\rangle$ allows to map the dual of $\mathcal{H}$ into the *tilde* space $\tilde{\mathcal{H}}$. Furthermore, as we shall see in the next section, the twin formulation permits a certain freedom (up to the gauge transformation) of the definition of the twin-space counterpart of the Liouville operator, which can be used to make mathematical formulations more compact and numerical simulations more efficient.

2.2 | Finite-temperature Schrödinger equation

TFD stems from the simple observation that an expectation value in the twin-space formalism can be cast into a wavefunction-like form using the identity

$$\langle A(t)\rangle = \langle I|A\rho(t)|I\rangle \equiv \left\langle I|A\rho(t)^{1/2}\rho(t)^{1/2}|I\right\rangle = \left\langle I|\tilde{\rho}(t)^{1/2}A\rho(t)^{1/2}|I\right\rangle = \langle\psi(t)|A|\psi(t)\rangle \tag{15}$$

where we have used the property of Equation (7), and the state vector

$$|\psi(t)\rangle = \rho(t)^{1/2}\,|I\rangle \tag{16}$$

satisfies the equation[45]

$$\frac{\partial}{\partial t}|\psi(t)\rangle = -i\hat{H}\,|\psi(t)\rangle \tag{17}$$

with the initial condition

$$|\psi(0)\rangle = \rho(0)^{1/2}\,|I\rangle. \tag{18}$$

Therefore the use of the twin space allows to recast all quantum statistical mechanics into a wave function theory in a double Hilbert space $\mathscr{L} = \left(\mathcal{H}\otimes\tilde{\mathcal{H}}\right)$. We notice that the density vector $|\rho(t)\rangle$ and the new wave function $|\psi(t)\rangle$ obey the same evolution equation but with different initial conditions.

Let us now consider a system that is prepared at thermal equilibrium at $t = 0$, that is,

$$\rho(0) = Z^{-1}e^{-\beta H} \tag{19}$$

Z being the partition function. We further observe that in most molecular systems the characteristic energy of electronic states are much higher than those of nuclear (vibrational) states, therefore we can assume that composite electron-vibrational system at ambient temperature resides in the ground state of the electronic subsystem (A), $|0_A\rangle$, and possesses thermal distribution over the DoFs of the vibrational subsystem (B), that is

$$\rho(0) = |\,0_A\rangle\langle 0_A\,|\,Z_B^{-1}e^{-\beta H_B}, \tag{20}$$

H_B being the vibrational Hamiltonian, in the ground electronic state, and Z_B the corresponding partition function. The assumption (20) is rooted into Born–Oppenheimer approximation, it has a huge number of applications in molecular physics and spectroscopy,[1] and is the key to the description of molecular aggregates,[46–48] electron-vibrational[49], and vibration-rotational[50] systems.

If the above assumption holds true, it is possible to show that Equation (17) can be rewritten in the equivalent form[51]

$$\frac{\partial}{\partial t}|\psi(t)\rangle = -i\bar{H}\,|\psi(t)\rangle \tag{21}$$

in which the new Hamiltonian operator, $\bar{H}$, is defined as

$$\bar{H} = H - \tilde{h}_B. \tag{22}$$

where $\tilde{h}_B$ is any operator acting in the tilde space of the vibrational subsystem, which can be chosen as an arbitrary gauge to help solve the mathematical problem. Equation (21) should be solved with the initial condition

$$|\psi(0)\rangle = |\,0_A\rangle\,|\,0_B(\beta)\rangle \tag{23}$$

where, according to Equation (18)

$$|0_B(\beta)\rangle = \rho_B(0)^{1/2}\,|I_B\rangle = Z_B^{-1/2} e^{-\beta H_B/2} \sum_{\boldsymbol{k}\in B} |\boldsymbol{k}\tilde{\boldsymbol{k}}\rangle. \tag{24}$$

in which $|\boldsymbol{k}\rangle$ labels the vibrational states of the original Hilbert space and $|\tilde{\boldsymbol{k}}\rangle$ the states of the corresponding fictitious *tilde* space. Therefore, the solution of the original Liouville - von Neumann equation for $\rho(t)$ with the initial condition (20) is reduced to the solution of the Schrödinger equation (21) in the extended vector space spanned by the basis $\{|\boldsymbol{n}\rangle \otimes |\boldsymbol{k}\rangle \otimes |\tilde{\boldsymbol{k}}\rangle\}$, where $|\boldsymbol{n}\rangle$ labels the electronic basis set of system A, and $\{|\boldsymbol{k}\rangle, |\tilde{\boldsymbol{k}}\rangle\}$ the physical and *tilde* vibrational basis sets, respectively. In this special formulation of TFD theory we have explicitly taken advantage of the separation of the energy ranges of the electronic and vibrational subsystems (Equation (20)), avoiding the use of tilde variables for the entire system and employing them only for the thermalized DoFs of subsystem B (cf. Refs. 52 and 53).

The thermal vacuum vector $|0_B(\beta)\rangle$ possesses multiple nonzero components, and its use in practical simulations can be rather difficult, requiring imaginary time propagation.[54–56] However, the key advantage of the present method lies in the possibility to have a compact analytical representation of the thermal vacuum $|0_B(\beta)\rangle$.[57] Indeed, instead of the solution of the Schrödinger Equation (21) with the initial condition (23) it is much more practical to introduce a unitary transformation e^{-iG} in the $\{|\boldsymbol{k}\rangle \otimes |\tilde{\boldsymbol{k}}\rangle\}$ subspace obeying the identity

$$e^{-iG}\,|0_B\tilde{0}_B\rangle = |0_B(\beta)\rangle \tag{25}$$

where $|0_B\tilde{0}_B\rangle$ is the ground state in the $\{|\boldsymbol{k}\rangle \otimes |\tilde{\boldsymbol{k}}\rangle\}$ subspace.

Equation (25) defines what can be called generalized thermal Bogoliubov transformation.[58] Its application to Equation (21) yields the transformed TFD Schrödinger equation

$$\frac{\partial}{\partial t}|\psi_\theta(t)\rangle = -i\bar{H}_\theta\,|\psi_\theta(t)\rangle \tag{26}$$

where

$$\bar{H}_\theta = e^{iG}\bar{H}e^{-iG}, \tag{27}$$

$$|\psi_\theta(t)\rangle = e^{iG}\,|\psi(t)\rangle \tag{28}$$

and the initial condition

$$|\psi_\theta(0)\rangle = |0_A\rangle\,|0_B\tilde{0}_B\rangle \tag{29}$$

corresponds to the global vacuum state. The expectation value of any operator A (acting in the physical, $\{|\boldsymbol{n}\rangle\otimes|\boldsymbol{k}\rangle\}$, vector space) can now be rewritten as

$$\langle A(t)\rangle = \langle\psi_\theta(t)|A_\theta|\psi_\theta(t)\rangle \quad \text{with} \quad A_\theta = e^{iG}Ae^{-iG}. \tag{30}$$

We underline that the expectation values evaluated via Equations (15) and (30) are identical. The TFD machinery with thermal Bogoliubov transformation gives an alternative representation of quantum mechanics which is fully equivalent to the traditional density–matrix representation.

The last step required to complete our theory is to provide an explicit analytical form of the thermal Bogoliubov transformation and a set of rules to obtain the transformed Hamiltonian operator $\bar{H}_\theta$. The explicit form of the transformation 25 is well known for two cases of notable interest, that is, for ensembles of free bosons and free fermions.[21–23,39,59] Extensions to more general systems can also be obtained although their practical use can be rather cumbersome.[51]

The problems we wish to tackle in this work require, in most cases, that the physical observable of interest be averaged over a thermalized ensemble of nuclear vibrations which are modeled as harmonic oscillator states, that is H_B of Equations (20) and (24) is

$$H_B = \sum_j \omega_j a_j^\dagger a_j, \tag{31}$$

where $a_j^\dagger$ (a_j) are the creation (annihilation) Bose operators ($\left[a_j, a_{j'}^\dagger\right] = \delta_{jj'}$) and ω_j are vibrational frequencies. The collection of vibrational DoFs that defines the above Hamiltonian operator includes both high frequency modes typical of molecular systems, and low frequency "environment" modes. After the seminal work of Caldeira and Leggett on quantum dissipative systems,[60] the importance of this model of the environment in various applications is hardly overestimated.

The operator of the thermal Bogoliubov transformation corresponding to the Hamiltonian of Equation (31) reads[22]

$$G = -i\sum_j \theta_j \left(a_j \tilde{a}_j - a_j^\dagger \tilde{a}_j^\dagger\right) \tag{32}$$

where

$$\theta_j = \operatorname{arctanh}\left(e^{-\beta\omega_j/2}\right). \tag{33}$$

Hence, thermal Bogoliubov transformation introduces thermal noise into the physical system by coupling it to the fictitious tilde system through the temperature-dependent mixing parameters θ_j.

If the Hamiltonian H and the operator $\tilde{h}_B$ are polynomials in creation-annihilation operators (which is the case in many real world applications) then the explicit form of $\bar{H}_\theta$ can be constructed by using the fundamental relations[22,53,61]

$$e^{iG} a_j e^{-iG} = a_j \cosh(\theta_j) + \tilde{a}_j^\dagger \sinh(\theta_j) \tag{34}$$

$$e^{iG} \tilde{a}_j e^{-iG} = \tilde{a}_j \cosh(\theta_j) + a_j^\dagger \sinh(\theta_j) \tag{35}$$

Therefore, the transformed Hamiltonian $\bar{H}_\theta$ depends on temperature through the parameters θ_j. Equations (26)–(35) are the working tools of our new approach to finite temperature quantum dynamics in molecular systems.

2.3 | Finite-temperature electron-vibrational Hamiltonian

Let us now focus on a special type of the Hamiltonian operator describing a set of coupled electronic states interacting with a phonon bath

$$H = \sum_{n=1}^{M} \varepsilon_n |n\rangle\langle n| + \sum_{n \neq m} V_{nm} |n\rangle\langle m| + \sum_{k=1}^{d} \omega_k a_k^\dagger a_k - \sum_{kn} \frac{g_{kn}}{\sqrt{2}} |n\rangle\langle n| \left(a_k^\dagger + a_k\right). \tag{36}$$

Here $|n\rangle$ labels an electronic state of the system with the energy ε_n, V_{nm} are electronic couplings, ω_k are the frequencies of the bath harmonic oscillators, and the parameters g_{nk} determine the strength of the electron–phonon coupling. The Hamiltonian (36) has a large number of applications, such as the fundamental description of molecular aggregates properties,[46–48] the analysis of molecular processes in the linear vibronic-coupling theory,[49,62] electron-transfer and charge-transfer properties in molecular systems.[11,63,64]

In what follows we choose the gauge of Equation (22) as

$$\tilde{h}_B = \sum_{k=1}^{d} \omega_k \tilde{a}_k^\dagger \tilde{a}_k. \tag{37}$$

Applying the Bogoliubov transformation to the Hamiltonian operator (36) we obtain the temperature-dependent operator

$$\bar{H}_\theta = e^{iG}\bar{H}e^{-iG} = \sum_n \varepsilon_n |n\rangle\langle n| + \sum_{n\neq m} V_{nm}|n\rangle\langle m| + \sum_k \omega_k \left(a_k^\dagger a_k - \tilde{a}_k^\dagger \tilde{a}_k\right)$$

$$-\sum_{kn}\frac{g_{kn}}{\sqrt{2}}\left\{\left(a_k + a_k^\dagger\right)\cosh(\theta_k) + \left(\tilde{a}_k + \tilde{a}_k^\dagger\right)\sinh(\theta_k)\right\}|n\rangle\langle n|. \tag{38}$$

In deriving the above expression we used the invariance property[22]

$$e^{iG}\left(a_n^\dagger a_n - \tilde{a}_n^\dagger \tilde{a}_n\right)e^{-iG} = a_n^\dagger a_n - \tilde{a}_n^\dagger \tilde{a}_n. \tag{39}$$

The operator $\bar{H}_\theta$ of Equation (38) consists of two parts: a modified physical Hamiltonian in which the linear coupling terms are multiplied by $\cosh(\theta_k)$ factors, and the vibrational tilde Hamiltonian. The excitation of the tilde vibrations is caused by the linear coupling terms $g_{kn}\sinh(\theta_k)$. Since $\tilde{h}_B$ enters Equation (38) with a negative sign, vibrational excitations in the tilde space correspond to a flow of energy from the physical system to the fictitious tilde system. It is this type of coupling that accounts for thermal noise. Once the explicit structure of $\bar{H}_\theta$ has been determined the evaluation of the expectation value of any observable $\langle A(t)\rangle$ can be obtained from Equation (30) after the solution of the TFD Schrödinger Equation (26).

The explicit dependence of the Hamiltonian operator on the temperature through the parameters θ_k enables a smooth transition from the low temperature to the high temperature case. At $T\to 0$ the mixing parameters θ_k become zero, $\sinh(\theta_k)\to 0$, the coupling to the tilde space disappears, and the standard Schrödinger equation is recovered as expected. For high-frequency modes, $\theta_k \ll 1$, $\sinh(\theta_k)\approx 0$, and $\cosh(\theta_k)\approx 1$ even at room temperature. As a rule of thumb high-frequency modes need not be incorporated into the tilde Hamiltonian. This leads to additional reduction of the active space and computational savings (see Section 4.3). This a priori selection of the DoFs which need doubling cannot be used within the standard formulation of the Liouville–von Neumann equation for the density matrix: in that case the bra and ket spaces have by construction the same dimensionality.

3 | TENSOR TRAINS

3.1 | Basic theory

The solution of the TFD Schrödinger Equation (26) with the Hamiltonian (38) requires efficient numerical methods, suitable to accurately treat a large number of dynamical variables. Several techniques have been developed which can, at least in principle, overcome what has been termed the *curse of dimensionality*.[3,15] In our approach the TT decomposition, the simplest form of Tensor Network, has been adopted. Below we sketch the basic principles of the TT decomposition, and show how it can be applied to solve the thermal Schrödinger equation in twin-formulation. The reader is referred to the original articles[3,35,65] for a detailed analysis of the TT theory.

Let us consider a generic state $|\psi\rangle$ of a N dimensional quantum system having the form

$$|\psi\rangle = \sum_{i_1, i_2, \ldots, i_N} C(i_1, \ldots, i_N)|i_1\rangle|i_2\rangle\cdots|i_N\rangle. \tag{40}$$

where $|i_k\rangle$ labels the basis states of the k-th dynamical variable, and the elements $C(i_1, \ldots, i_N)$ are complex numbers labeled by N indices. If we truncate the summation of each index i_k the elements $C(i_1, \ldots, i_N)$ represent a tensor of order N, where the word "order" means nothing but the number of DoFs. The evaluation of Equation (40) requires the computation (and storage) of p^N terms, where p is the average size of the one-dimensional basis set that is usually much larger than 2, becoming therefore prohibitive for large N. Using the TT format, each element $C(i_1, \ldots, i_N)$ of the tensor C is approximated as

$$C(i_1, \ldots, i_N) \approx C_1(i_1)C_2(i_2)\cdots C_N(i_N) \tag{41}$$

where each $C_k(i_k)$ is a $r_{k-1} \times r_k$ complex matrix. In the explicit index notation

$$C(i_1, ..., i_N) = \sum_{\alpha_0 \alpha_1 \cdots \alpha_N} C_1(\alpha_0, i_1, \alpha_1) C_2(\alpha_1, i_2, \alpha_2) \cdots C_N(\alpha_{N-1}, i_N, \alpha_N) = \sum_{\{\alpha_k\}} \prod_{k=1}^{N} C_k(\alpha_{k-1}, i_k, \alpha_k) \tag{42}$$

The matrices C_k are three dimensional arrays, called *cores* of the TT decomposition. The dimensions r_k are called compression ranks. Since the product of Equation (41) must be a scalar, the constraint $\alpha_0 = \alpha_N = 1$ must be imposed. In the matrix-product state (MPS) language the sizes of the ranks are referred to as *bond dimensions*. Using the TT decomposition 41 it is possible, at least in principle, to overcome most of the difficulties caused by the dimensionality of the problem. Indeed, the wave function is entirely defined by N arrays of dimensions $r_{k-1} \times n_k \times r_k$ thus requiring a storage dimension of the order Npr^2. The meaning of the term Tensor Train can be easily understood by looking at the graph of Figure 1.

We notice that if all the ranks of the cores are 1, the TT format is equivalent to a Kronecker product. From this point of view it constitutes the simplest extension of a direct product to entangled systems. The higher the entanglement, that is the correlation between two or more DoFs, the larger the ranks of the TT cores connecting their respective indices. Indeed, a fundamental problem of the TT representation is to define the sequence of indices i_k, $k = 1, ..., N$ with the minimum rank decomposition of the state vector, and of the operators. We do not aim to tackle this complex mathematical problem, however we can exploit the twin-space formalism to optimize the TT representation of the vector $|\psi(t)\rangle$.

The algebra of tensor trains has been thoroughly discussed elsewhere and efficient algorithm exists to perform basic operations such as scalar and matrix–vector products. For completeness here we briefly describe some of the basic operations, and refer the reader to more technical articles for details.[35]

The addition of two vectors A and B in TT format

$$A = A_1(i_1) A_2(i_2) \cdots A_N(i_N); \quad B = B_1(i_1) B_2(i_2) \cdots B_N(i_N) \tag{43}$$

can be easily implemented by merging the cores as in a direct sum. The cores of the new tensor $C = A + B$ will be

$$C_k(i_k) = \begin{pmatrix} A_k(i_k) & 0 \\ 0 & B_k(i_k) \end{pmatrix} \; k = 2, ..., N-1 \tag{44}$$

$$C_1(i_1) = (A_1(i_1) \; B_1(i_1)); C_N(i_N) = \begin{pmatrix} A_N(i_N) \\ B_N(i_N) \end{pmatrix} \tag{45}$$

It follows that if the matrices $A_k(i_k)$ and $B_k(i_k)$ have ranks $r_{k'}$ and $r_{k''}$, respectively, the rank of the core $C_k(i_k)$ will be $r_k = r_{k'} + r_{k''}$. This increase in the ranks upon addition is a fundamental problem which is usually addressed by rounding the new TT with a prescribed accuracy (see Section 3.2).

Matrix-by-vector multiplication is certainly one of the most important operations in linear algebra. In the many-dimensional case this operation requires the contraction over a set of indices in the form

$$A(i_1, ... i_N) = \sum_{j_1, \cdots, j_N} X(i_1, .., i_N; j_1, ... j_N) B(j_1, ..., j_N). \tag{46}$$

The tensor X is said to be in TT-format if it is represented as

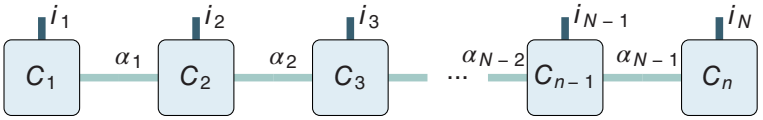

FIGURE 1 Graphical representation of a tensor train. Each square node represents a core of the TT, and each vertical line represents an index i_k of the tensor. Connecting lines represent the contractions over the indices α_k

$$X(i_1,..,i_N;j_1,...j_N) = X_1(i_1,j_1)X_2(i_2,j_2)\cdots X_N(i_N,j_N) \tag{47}$$

where $X_k(i_k,j_k)$ are $r_{k-1}\times r_k$ matrices, that is, in the explicit index notation

$$X(i_1,..,i_N;j_1,...j_N) = \sum_{\alpha_0\alpha_1\ldots\alpha_N} X_1(\alpha_0,i_1,j_1,\alpha_1)X_2(\alpha_1,i_2,j_2,\alpha_2)\cdots X_N(\alpha_{N-1},i_N,j_N,\alpha_N) \tag{48}$$

If the vector B is in TT format then we have

$$\begin{aligned} A(i_1,\ldots i_N) &= \sum_{j_1,\ldots j_N} (X_1(i_1,j_1)\cdots X_N(i_N,j_N))(B_1(j_1)\cdots B_N(j_N)) \\ &= \sum_{j_1,\ldots j_N} (X_1(i_1,j_1)\otimes B_1(j_1))\cdots(X_N(i_N,j_N)\otimes B_N(j_N)) \\ &= A_1(i_1)\cdots A_N(i_N) \end{aligned} \tag{49}$$

In this operation each core X_k acts separately on the cores B_k of the vector B. We notice that the TT-ranks of the resulting vector A are the product of ranks of the matrix and of the vector. This latter result severely limits the numbers of consecutive matrix-by-vector multiplications that can be performed and implies that after a multiplication a TT-rounding must be performed to avoid rank growth.

3.2 | Tensor-train rounding

Suppose that the tensor A is in the TT-format

$$A = A_1(i_1)A_2(i_2)\cdots A_N(i_N) \tag{50}$$

with core ranks r_k. This tensor can be for example the result of the addition of several tensors and therefore the ranks r_k can be particularly large. To avoid waste of computer memory and time it is desirable to approximate A with a new tensor B in TT format such that

$$\|A-B\|_F \le \epsilon\|A\|_F \tag{51}$$

Such a procedure is called rounding. The new tensor B will have ranks $r_{k'} \le r_k$ while maintaining the prescribed accuracy ϵ. This problem is well known in the theory of TT decomposition and can be elegantly solved performing a sequence of singular value decompositions (SVD) of each core of the original tensor A retaining only singular values above a predefined threshold. The reader is referred to the original article for details about the implementation.[35]

3.3 | Vibronic Hamiltonian operator in tensor-train format

In order to apply TT representation to solve the time-dependent Schrödinger Equation (21) both the state vector and the Hamiltonian operator have to be represented in TT format. The construction and storage of the Hamiltonian operator of Equation (36) in TT format can be performed by a sequence of additions of TT matrices followed by a rounding to keep the ranks to a reasonable value. If M is the number of electronic states and p_k is the size of the truncated basis set for the k-th vibrational DoF the Hamiltonian operator (38) has the matrix form

$$\mathbf{H} = \mathbf{H}_e\otimes\mathbf{I}_1\cdots\mathbf{I}_d + \sum_k \omega_k(\mathbf{I}_e\otimes\cdots\mathbf{W}_k\cdots\otimes\mathbf{I}_d) - \sum_{kn} g_{kn}(\mathbf{S}_{en}\otimes\mathbf{I}_1\cdots\mathbf{Q}_k\cdots\mathbf{I}_d) \tag{52}$$

where $\mathbf{H}_e$ is the electronic Hamiltonian matrix

$$\mathbf{H}_e = \begin{pmatrix} E_1 & V_{12} & \cdots \\ V_{21} & \ddots & \\ \vdots & & E_M \end{pmatrix}, \tag{53}$$

$\mathbf{Q}_k$ and $\mathbf{W}_k$ are the coordinate and energy matrices of mode q_k in its energy eigenbasis representation

$$\mathbf{Q}_k = \frac{1}{\sqrt{2}} \begin{pmatrix} 0 & \sqrt{1} & \cdots \\ \sqrt{1} & & \sqrt{p_k - 1} \\ \vdots & \sqrt{p_k - 1} & 0 \end{pmatrix}; \quad \mathbf{W}_k = \begin{pmatrix} 0 & & \\ & 1 & \\ \vdots & & p_k - 1 \end{pmatrix}, \tag{54}$$

$\mathbf{I}_e$ is a unit matrix of size $M \times M$, $\mathbf{S}_{en}$ is the matrix representation of the $|n\rangle\langle n|$ electronic operator, and $\mathbf{I}_k$ are identity matrices of size $(p_k \times p_k)$, $k = 1, ..., d$.We now wish to provide a TT approximation, $\mathbf{H}_\varepsilon$ of the Hamiltonian matrix (52) of the type

$$\mathbf{H}_\varepsilon(i_1, \ldots i_N; j_1, ..., j_N) = \mathbf{H}_1(i_1, j_1)\mathbf{H}_2(i_2, j_2) \cdots \mathbf{H}_N(i_N, j_N) \tag{55}$$

such that

$$\|\mathbf{H} - \mathbf{H}_\varepsilon\|_F \leq \varepsilon \|\mathbf{H}\|_F. \tag{56}$$

To this end we observe that each direct product in Equation 52 is a tensor train with all ranks $r_k = 1$, therefore their sum can be easily obtained using the rules of Equation 44. Since after addition the ranks of TT cores increase it is necessary to perform a TT rounding after each operation. Algorithm 1 describes the pseudocode for obtaining the *TT* approximation of the vibronic Hamiltonian matrix (52) with a prescribed accuracy ϵ.

Algorithm 1: Computation of the vibronic Hamiltonian of eq. 36 in TT format. The algorithm requires the function *tt_add* to perform addition of two arrays in TT format and the function *tt_round* for rounding a TT array to a prescribed accuracy ϵ. The function *tt_matrix* serves only as a type definition and constructs a TT tensor from its cores.

Data: $\mathbf{H_e}$,$\mathbf{S}_{en}$, $\{g_{nk}, \omega_{nk}, \mathbf{Q}_k, \mathbf{W}_k, \mathbf{I}_k, r_k, p_k\}$ for $k = 1, ..., d$
Result: Hamiltonian operator in TT format:
$\mathbf{H}_\epsilon(i_1, ..., j_N) = \mathbf{H}_1(i_1, j_1)\mathbf{H}_2(i_2, j_2) \cdots \mathbf{H}_N(i_N, j_N)$
$\mathbf{H} := tt\_matrix(\mathbf{H}_e, \mathbf{I}_1, \cdots, \mathbf{I}_d)$ // initialize TT-format $\mathbf{H}$ matrix
for $k = 1$ **to** d **do**
  $\mathbf{T} := \omega_k \times tt\_matrix(\mathbf{I}_e, \cdots \mathbf{W}_k, \cdots, \mathbf{I}_d)$
  $\mathbf{H} := tt\_add(\mathbf{H}, \mathbf{T})$ // addition of two arrays in TT format
  $\mathbf{H} := tt\_round(\mathbf{H}, \epsilon)$ // rounding of a TT matrix
for $n = 1$ **to** M **do**
  for $k = 1$ **to** d **do**
    $\mathbf{T} := g_{nk} \times tt\_matrix(\mathbf{S}_{en}, \cdots \mathbf{Q}_k, \cdots, \mathbf{I}_d)$
    $\mathbf{H} := tt\_add(\mathbf{H}, \mathbf{T})$ // addition of two arrays in TT format
    $\mathbf{H} := tt\_round(\mathbf{H}, \epsilon)$ // rounding of a TT matrix
return $\mathbf{H}(i_1, ..., j_N) := \mathbf{H}_1(i_1, j_1), \mathbf{H}_2(i_2, j_2), \cdots, \mathbf{H}_N(i_N, j_N)$

3.4 | Application of tensor trains to time-dependent problems

In a time-dependent theory the cores are time-dependent complex matrices which must be determined from the numerical solution of the equations of motion of the system.[36,66,67] The simplest possible approach to tackle this problem is to

use standard integrators of systems of ordinary differential equations (ODEs) combined with the algebra of tensor trains. Let us assume that the wave function can be represented as

$$|\psi(t)\rangle = \sum_{i_1, i_2, \ldots, i_N} C_1(i_1;t)C_2(i_2;t)\cdots C_N(i_N;t)\,|\,i_1\rangle\,|\,i_2\rangle\cdots|\,i_N\rangle \tag{57}$$

and that H is the Hamiltonian operator in TT format that controls its evolution. We could use a forward Euler scheme and obtain the solution of Equation (21) in the form

$$C(i_1, \ldots, i_N; t+\tau) = C(i_1, \ldots, i_N; t) - i\tau\hat{H}C(i_1, \ldots, i_N; t) + O(\tau^2). \tag{58}$$

As described in the preceding section the ranks of the cores of the vector $y = HC$ are obtained by multiplying the ranks of H and those of C, and the sum $C - i\tau HC$ results in a further increase of the ranks of the final vector. This scheme therefore requires an efficient rounding procedure after each time step. Almost always the truncation scheme allows for an a priori upper bound of the ranks r_k. This truncation, however, results in artificial changes of the total energy and of the norm of wave function under unitary evolution. The so-called Time-Evolving Block Decimation (TEBD) technique, the Krylov subspace methods[68–70] belong to this class of methods. A recent implementation of the second-order Cranck–Nicholson integrator combined with the Alternating-Minimal-energy solver of linear systems in TT format has been proposed to control the increase in the ranks of the cores.[67]

An alternative approach to tackle this problem is to apply the time-dependent variational principle (TDVP) to the parameterized form of the state given by Equation (57).[71] Since TTs of fixed rank form a closed manifold $\mathcal{M}_{TT}$ the resulting equations of motion can be written in the form

$$\frac{d}{dt}|\,\psi(C(t))\rangle = -i\hat{P}_{T(C(t))}H\,|\,\psi(C(t))\rangle, \tag{59}$$

where C labels all the cores of the TT representation (57), and $\hat{P}_{T(\psi(C(t)))}$ is the orthogonal projection into the tangent space of $\mathcal{M}_{TT}$ at $|\psi(C(t))\rangle$. Equation (59) provides an approximate solution of the original equation on the manifold of TT tensors of fixed rank, $\mathcal{M}_{TT}$.[65] This means that the projected evolution gives the best solution with a prescribed upper bound for the ranks of cores. This strategy is extremely appealing because it avoids, by construction, the growth of the ranks of the TT solution. The drawback of the methodology is that the accuracy of the solution must be verified a posteriori. This requires several calculations, with increasing the values of the ranks r_k, to be performed, until a global convergence on a desired observable is reached.

We refer the reader to references,[36,72] where the explicit differential equations are derived and their approximation properties are analyzed, and to Ref. 73 for a discussion of time-dependent TT/MPS approximations in the theoretical physics literature.

In Sections 4 and 5.3 we employ the TDVP algorithm, and show how to control the behavior of the solution as a function of the average value of the ranks.

3.5 | Entanglement growth and structure of the tensor train

The TT approximation is effective only if the ranks r_k of the cores are small. The structure of the train, that is the order of the indices of the tensor, can have a deep impact on the growth of the entanglement. A key aspect is that if two DoFs are highly entangled their indices should be as close as possible in the sequence that defines the TT representation of the wave function. The most desirable situation would correspond to a systems showing only nearest neighbor interactions and a structure of the tensor train that reflects the natural form of the Hamiltonian operator. This latter is dictated by the structure of the problem under examination, but several techniques exist to map the Hamiltonian of Equations (36) and (38) to chain-like models, thus easing the application of the TT format.[74–76] Yet, it has been recently demonstrated that this mapping might not be necessary at all, and sometime can even be counterproductive.[77] In all the applications presented in Section 4 we have found that ordering the electronic and vibrational DoFs of the Hamiltonian in Equation (27) with increasing values of their

frequency ω_i provides very good convergence properties of the TT representation, and the mapping to a chain form is not required.

4 | APPLICATIONS

The TFD-TT approach can be applied to study the time evolution of quantum observables of a wide range of chemico-physical systems. Below we describe some applications both to the study of model systems as well as to the characterization of energy and electron transfer problems in realistic many-dimensional molecular systems.

The Hamiltonian operators of all systems considered in this section are particular cases of the Hamiltonian of Equation (36) and of the thermal Hamiltonian of Equation (38).

4.1 | Model systems

4.1.1 | Spin-boson model

Starting from the general Hamiltonian of Equation 36 we have studied a prototypical spin-boson system[9] in which two degenerate electronic states, $|1\rangle$ and $|2\rangle$, are coupled to low frequency vibrational modes

$$H = \epsilon\sigma_z - V\sigma_x + \sum_k \omega_k a_k^\dagger a_k + \sigma_z \sum_k g_k \left(a_k^\dagger + a_k\right) \tag{60}$$

where, as usual, $\sigma_z = (|1\rangle\langle 1| - |2\rangle\langle 2|)$ and $\sigma_x = (|1\rangle\langle 2| + |2\rangle\langle 1|)$, 2ϵ is the electronic energy difference between the two states, V is the electronic coupling, and the constants g_k are responsible for the linear coupling between the ensemble of bosons of frequencies ω_k and the spin. These parameters can be modeled starting from the so-called spectral density function, defined as

$$J(\omega) = \sum_k g_k^2 \delta(\omega - \omega_k). \tag{61}$$

In our model the Ohmic spectral density is employed

$$J(\omega) = \frac{\pi}{2}\alpha\omega e^{-\omega/\omega_c} \tag{62}$$

with a cut-off frequency $\omega_c = 53\ \mathrm{cm}^{-1}$. The solution of Equation (26) using a basis set representation requires the discretization of the spectral density over a finite set of frequencies. We have adopted a non-uniform discretization procedure that ensures fast convergence with respect to the number of sampling points in which the frequencies and the coupling parameters are given by:[78]

$$\omega_k = -\omega_c \ln(1 - k\Omega/\omega_c);\ g_k = \alpha\omega_k\Omega;\ \Omega = \frac{\omega_c}{d}\left(1 - e^{-\omega_{max}/\omega_c}\right);\ k = 1, \ldots, d \tag{63}$$

In our calculations the spectral density is discretized with $d = 200$ DoFs in the range $(0{,}5\omega_c]$.

Figure 2 shows the population $P(t)$ of the initial upper electronic state at 300 K for the set of parameters reported in the caption. The TFD-TT results correspond to the full lines, while the blue dots correspond to the numerically exact populations computed in Ref. 79 via the HEOM methodologies (HEOM is a standard reference for benchmarking high-temperature simulations). Clearly, the TFD-TT and HEOM populations are in excellent agreement and virtually indistinguishable. The comparison unequivocally demonstrates the validity of the TFD-TT approach for this type of quantum dynamical problems.

The convergence properties of the numerical methodology are illustrated by Figure 3 which shows the population as a function of time for different values of the TT compression ranks. At a low temperature, $T = 30$ K, the convergence

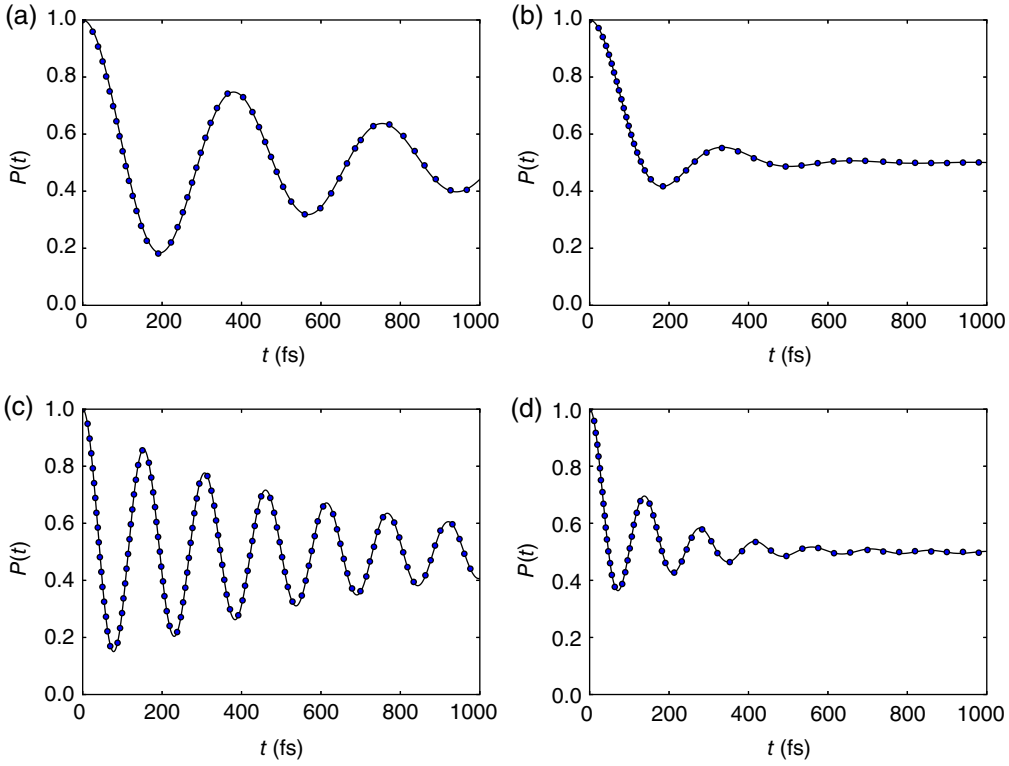

FIGURE 2 Population $P(t)$ of the initial electronic state at $T = 300$ K as a function of time, for different values of $\alpha = \lambda/(2\omega_c)$; (a) $\lambda = 5\,\mathrm{cm}^{-1}$; (b) $\lambda = 20\,\mathrm{cm}^{-1}$ (both with the tunneling amplitude $V = 40\,\mathrm{cm}^{-1}$); (c) $\lambda = 20$; (d) $\lambda = 80$ (both with $V = 100\,\mathrm{cm}^{-1}$). Full lines: TFD-TT calculations. Blue dots: Numerically exact HEOM calculations of Ref. 79

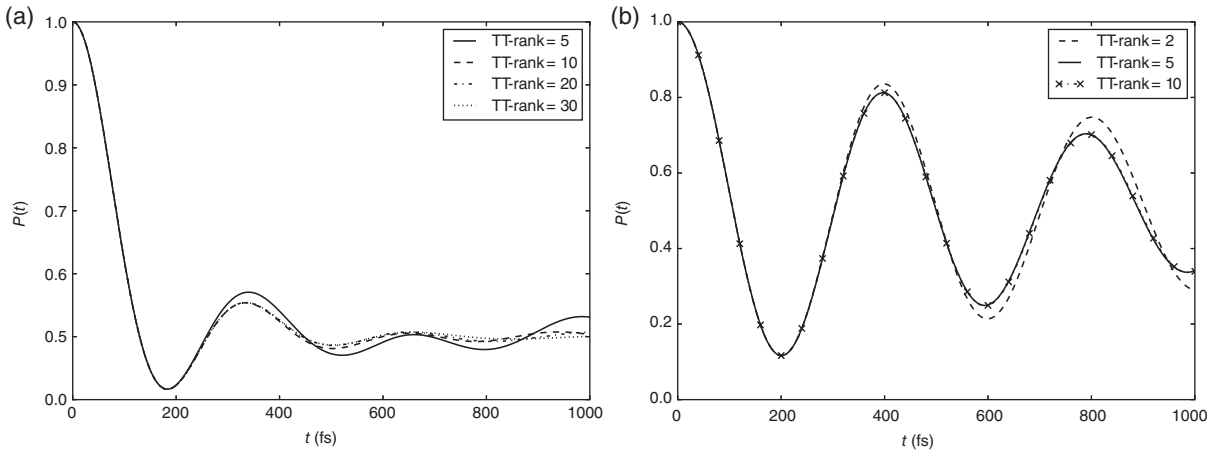

FIGURE 3 Population $P(t)$ of the initial electronic state as a function of time for different values of the TT compression ranks simulated for $\alpha = (20\,\mathrm{cm}^{-1})/(2\omega_c)$ and $V = 40\,\mathrm{cm}^{-1}$. (a) $T = 300$ K; (b) $T = 30$ K

is achieved with very low compression ranks, while at higher temperature higher ranks are required. Since the required TT storage scales quadratically with the average TT rank, this amounts to an increased computational cost of the calculation.

4.1.2 | Reaction mode spin-boson

One of the key advantages of using a basis set approach is the possibility to describe a large variety of potential energy surfaces beyond linear electron–phonon couplings. This is important for the description of chemical reactions in which

the surfaces can be highly anharmonic. In the following example the TFD-TT technique is used to study a system with bilinear couplings between electron and phonons.[9] We consider a system of two electronic states coupled to a single harmonic mode with the frequency Ω which is in turn coupled to a set of harmonic oscillators having Ohmic spectral density. The corresponding Hamiltonian, often referred to as reaction mode spin-boson,[80] can be written as

$$H = \epsilon\sigma_z - V\sigma_x + \Omega A^\dagger A + \sum_k \omega_k a_k^\dagger a_k + g\left(A^\dagger + A\right)\sigma_z + \left(A^\dagger + A\right)\sum_k \lambda_k\left(a_k^\dagger + a_k\right)\sigma_z. \tag{64}$$

where A, a_k ($A^\dagger, a_k^\dagger$) denote the annihilation (creation) operators for the reaction and bath oscillators respectively, and the couplings coefficients λ_k satisfy the relation

$$J(\omega) = \sum_k \lambda_k^2 \delta(\omega - \omega_k) = \frac{\pi}{2}\alpha\omega e^{-\omega/\omega_c}. \tag{65}$$

The value of the parameter g determines the strength of the coupling between the high frequency mode and the electronic subsystem. In this model the phonons "drain" energy from the reaction coordinate and not directly from the spin system. As in the previous case the continuous spectral density has been discretized using 200 vibrations; and the frequencies ω_k and couplings λ_k are obtained from Equation (63).

In Figure 4 the electronic population $P(t)$ at 30 K and 300 K is shown for two different values of the Kondo parameter α of Equation (65) (see figure caption for the Hamiltonian parameters).

At 30 K and small α the boson bath is not very effective in dissipating energy from the reaction coordinate. In this regime coherent oscillations of the electronic population persist at long times. When temperature increases to 300 K the damping is more evident but the oscillations remain underdamped. For larger α, the population at 30 K exhibits underdamped oscillations, while for 300 K the bath quenches the beatings at around 600 fs. The trend is natural, since the Kondo parameter controls the coupling of the reaction mode to the harmonic bath. The high-frequency modulation of the population dynamics is due to coherent vibrations of the reaction mode with a period $2\pi/\Omega \approx 22$ fs.

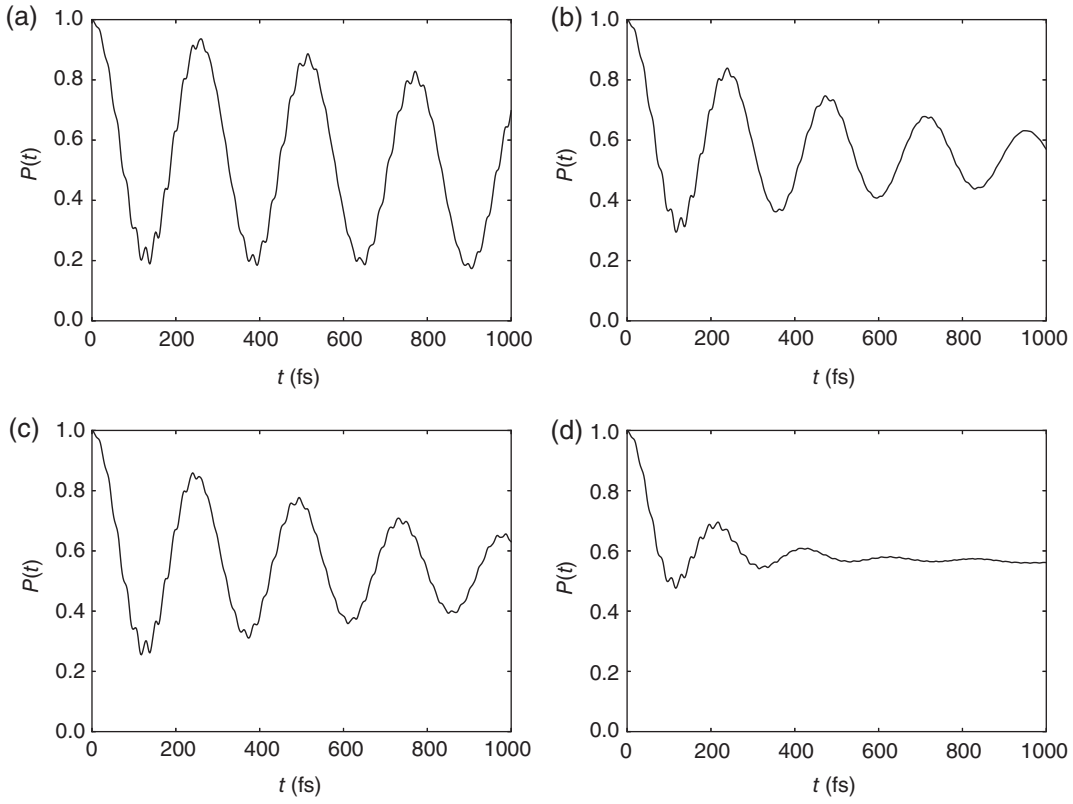

FIGURE 4 The time evolution of the electronic population $P(t)$, for different values of $\alpha = \lambda/(2\omega_c)$ and for a tunneling amplitude $V = 40\,\mathrm{cm}^{-1}$; (a) $\lambda = 20\,\mathrm{cm}^{-1}$, $T = 30$ K; (b) $\lambda = 20\,\mathrm{cm}^{-1}$, $T = 300$ K; (c) $\lambda = 80\,\mathrm{cm}^{-1}$, $T = 30$ K; (d) $\lambda = 80\,\mathrm{cm}^{-1}$, $T = 300$ K

4.2 | Energy transfer in supra-molecular assemblies

In the two preceding examples the vibronic couplings are derived from analytical functions which were devised to mimic mostly the behavior of low frequency vibrations of condensed phase systems. However, in most molecular systems this description does not hold, indeed, quite often the spectral densities are extremely structured, that is, absolutely not uniform. Providing an accurate description of finite temperature quantum dynamics in these systems can be a very challenging problem for most methodologies.

In recent works[10,81] we have shown how the TFD-TT methodology can be applied to the study exciton dynamics in the Fenna–Matthews–Olson (FMO) complex, consisting of seven bacteriochlorophylls (BChl) embedded into a protein matrix. This type of problem can indeed be described by using the general model Hamiltonian of Equation (36).

The exciton part of the FMO Hamiltonian, the site energies ε_n and electronic couplings V_{nm}, have been retrieved from Ref. 82. Vibronic coherences are essentially determined by the distribution of the bath vibrational frequencies and their coupling constants g_{kn}. For numerical convenience these parameters are assumed to be the same for all BChls ($g_{kn} = g_k$). Recent theoretical analysis suggest that the use of a "structured" spectral density in the energy transfer process can lead to quite pronounced vibronic effects.[5,83–85] Therefore, following Schulze et al.,[84] we have modeled the electron–phonon interaction by discretizing the experimental spectral density of Ref. 86 with $d = 74$ vibrations uniformly distributed in the range (2300 cm^{-1}). This way the times corresponding to the frequency $\omega_{\min} = 2\,\mathrm{cm}^{-1}$ and the line spacing $\Delta\omega = (\omega_{\max} - \omega_{\min})/d$ are safely beyond the observed time evolution of the system. We notice that using this spectral density the overall number of physical and tilde vibrational DoFs is 1038 ($14d$). We are not aware of any simulation at finite temperature with such a large number of DoFs.

The parameters $g_{kn}\cosh(\theta_k)$ and $g_{kn}\sinh(\theta_k)$ entering the thermal Hamiltonian $\bar{H}_\theta$ govern the coupling of the electronic subsystem with physical and *tilde* bosonic DoFs. Hence, it is tempting to introduce the spectral densities

$$J_p(\omega) = \sum_k (g_{kn}\cosh(\theta_k))^2 \delta(\omega - \omega_k), \quad J_t(\omega) = \sum_k (g_{kn}\sinh(\theta_k))^2 \delta(\omega + \omega_k), \tag{66}$$

which describe the electron-vibrational couplings in the physical (subscript p) and tilde (subscript t) subspace. As temperature goes to zero, $J_p(\omega) \to J(\omega)$ and $J_t(\omega) \to 0$. The two spectral densities are reported in Figure 5 at 77 K and 300 K. The comparison of lower and upper panels of the figure reveals how effective electron-vibrational coupling increases with temperature, notably for lower-frequency modes.

Figure 6(a) shows the total time-dependent populations $p_n(t)$ of seven ($n = 1 - 7$) BChl molecules of the FMO complex (standard numbering of the FMO cofactors is used). The populations are evaluated by Equations (30) and (26) for $A = A_\theta = |n\rangle\langle n|$ so that $p_n(t) = \langle A(t)\rangle$. The initial excitation is assumed to be localized on site 1. In all panels, $p_1(t)$ and $p_2(t)$ exhibit pronounced oscillations, as expected.[87,88]

At $T = 0$ K (upper panel) the populations are in perfect agreement with the results obtained by Schulze et al. using ML-MCTDH.[84] At $T = 77K$ (middle panel) $p_3(t)$ drops to about 0.6 at $t = 1$ ps. On the other hand, there is no pronounced difference in the behaviors of $p_1(t)$ and $p_2(t)$ at $T = 0$ and 77 K. In the language of spectral densities of Equation 66, it means that the contributions of the lower-frequencies vibrational modes (which are strongly

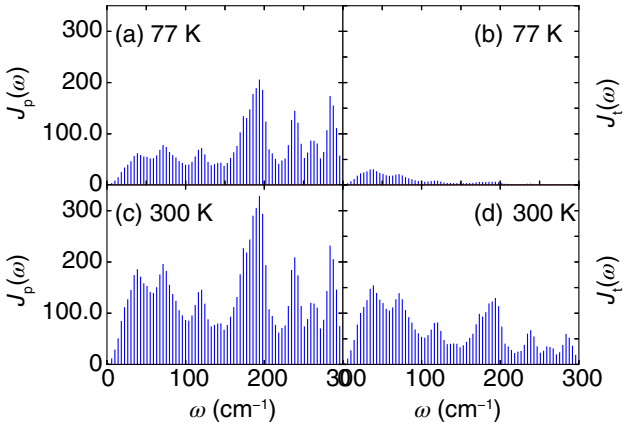

FIGURE 5 Effective site spectral densities $J_p(\omega)$ and $J_t(\omega)$ describing the coupling of the physical and tilde bosonic DoFs with the electronic subsystem at different temperatures. (a,b) 77 K, (c,d) 300 K

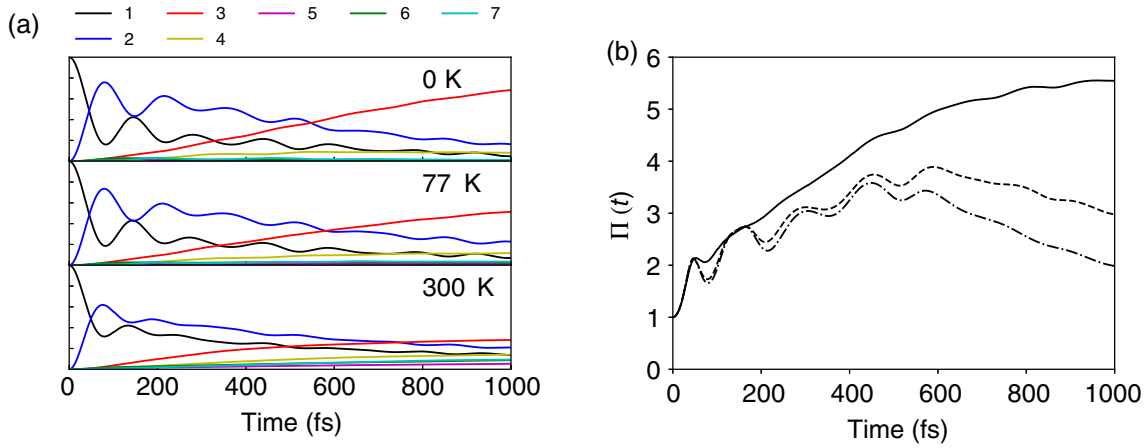

FIGURE 6 (a) Time evolution of the electronic populations $p_n(t)$ of seven ($n = 1 - 7$) BChl molecules of the FMO complex at different temperatures indicated in the panels. The initial excitation is localized on site 1. Different colors label different sites as specified in the legend. (b) Inverse participation ratio $\Pi(t)$ as a function of time; (−) 300 K, (−−) 77 K, (−·) 0 K

temperature-dependent) are quite significant in the dynamics of $p_3(t)$ at already 77 K, while are less pronounced in the dynamics of $p_1(t)$ and $p_2(t)$.

If temperature increases up to 300 K (lower panel) $p_3(t)$ further decreases to 0.3 at $t = 1$ ps, and the oscillatory components of $p_1(t)$ and $p_2(t)$ are significantly reduced but still visible. Such long-lived beatings at ambient temperature have not been reported in models employing an approximate spectral density in the Drude–Lorentz form,[87] Ohmic form or Adolphs–Regner (single peak) form.[88] The beatings revealed in the present work at $T = 300$ K are due to the strongly structured spectral density and frequency-dependent coupling between the electronic subsystem and the vibrational DoFs.

To elucidate how the spectral densities of Figure 5 affects the fraction of BChls that are significantly occupied during the time evolution of the system, we have computed the inverse participation ratio $\Pi(t)$, defined as[46,89]

$$\Pi(t) = \frac{1}{\sum_n p_n^2(t)}. \tag{67}$$

It is easy to show that $\Pi(t) = 1$ for a completely localized exciton wavefunction, while $\Pi(t) = N_{\text{site}}$ (7 in the present case) for a perfectly uniform state. Therefore, $\Pi(t)$ can be considered as an effective length, measuring the spatial extent of the exciton wave function over the aggregate. Figure 6(b) shows the computed $\Pi(t)$ for the FMO complex at different temperatures. At $T = 0$ K, $\Pi(t)$ has a strong quantum behavior showing an oscillatory increase for the first 400 fs which is followed by an oscillatory decrease to a value of 2 at $t = 1$ ps. This is an indication of the exciton self-trapping. Therefore, a small number of sites are accessible to the systems during its evolution at $T = 0$ K, as is also evident from the population dynamics in Figure 6(a). For $T = 77$ K, the qualitative behavior of $\Pi(t)$ remains the same but, the number of accessible sites increases to 3 at $t = 1$ ps. At ambient temperature the number of accessible sites increases significantly and the effective length of the exciton is about 5.5 at $t = 1$ ps. The effect of a finite temperature is thus not only to provide a decoherence mechanism but also to increase the number of sites simultaneously accessible for the energy transfer process and to destroy the exciton self-trapping (cf. Ref. 89).

4.3 | Electron-transfer in photosynthetic reaction centers

One of the key advantages of the TFD-TT methodology developed in Section 2 is that it can combine the best of wavefunction and density-matrix approaches into a single theoretical framework. Indeed, in our formulation the tilde space comprises only thermalized low frequency DoFs, therefore whenever the thermal mixing parameter θ of Equation (33) falls below a certain threshold the corresponding *tilde* variable is totally disentangled from the evolution of the physical system and can be omitted from the dynamical problem (see also Equation (29)).

The application of TFD-TT to the study of the dynamics of the electron-transfer (ET) between the accessory bacteriochlorophyll (B_A) and the bacteriopheophytin (H_A) in bacterial reactions centers,[11] clearly shows this special feature of the methodology.

Previous numerical studies have shown that this process can be modeled as a radiationless transition which involves mainly intramolecular vibrations which carry most of the reorganization energy.[19,64] However, quantum dynamical results were obtained only for models including a reduced space of nuclear vibrational coordinates, and the effect of finite temperature was not taken into account.[19]

Following a common approach,[90,91] the ET process is described by the Hamiltonian of Equation (36) with only two states, $|A\rangle, |F\rangle$ to describe the electronic subsystem. These latter are represented by the direct product of the neutral and anionic forms of the two isolated molecules, that is, $|A\rangle = |B_A^-\rangle\,|H_A\rangle$ and $|F\rangle = |B_A\rangle\,|H_A^-\rangle$. The Hamiltonian (36) can then be rewritten in the form

$$H = \epsilon_A\,|A\rangle\langle A| + \epsilon_F|F\rangle\langle F| + V(|A\rangle\langle F| + \text{H.c.}) + |F\rangle\langle F|\sum_k g_k\left(a_k + a_k^\dagger\right) + \sum_k \omega_k a_k a_k^\dagger \tag{68}$$

where ϵ_A, ϵ_F are the electronic energies of the states $|A\rangle$, $|F\rangle$ respectively, V is their electronic coupling. The linear vibronic couplings g_k can be obtained from the computation of the equilibrium geometry, and of the matrices of normal modes of vibrations of the two electronic states via well-known relations.[92–95] Our model comprises 267 vibrational modes, and the parameters adopted in here are taken from our previous work.[96]

Figure 7 shows the temperature-dependent spectral densities defined in Equation (66). As already said, the coupling with the tilde space is negligible for high frequency modes ($\omega > 2000\,\text{cm}^{-1}$) and not reported. It is immediate to see that as temperature increases the coupling with the low frequency part of the spectrum increases, while the high frequency region is left almost unaffected. This observation enables to analyze the relevance of temperature effects for each single degree of freedom and to reduce the computational costs by a priori removing some of the tilde DoFs from the Hamiltonian.

In the present case the physical number of DoFs is 267, which should be doubled to 534 upon inclusion of the tilde space. However, a large fraction of high frequency modes has a negligible vibronic coupling, $g_k\sinh(\theta_k)$, thus it is possible to reduce the overall number of nuclear DoFs to 400 without any loss in the accuracy of the model.

Figure 8(a) shows the convergence behavior of the TT methodology for different ranks of the cores. For sake of simplicity all cores have the same ranks, although different values are, in principles, allowed. As can be seen, the small rank approximation provides a good description of the dynamics only for short times. More specifically for $r = 10$ the dynamics is accurate up to 60 fs, while for $r = 20$ the dynamics is in almost quantitative agreement with the exact result up to 250 fs. Increasing r to 60 provides only slight modifications in the long-time tail of the decay. Indeed, after 800 fs the discrepancies between the population decay curves with $r = 60$ and $r = 50$ have an average relative deviation of about 5%. In all the calculations a basis set of harmonic oscillator eigenfunctions has been used with maximum quantum number 20 for all the DoFs, which guarantee converged results.[11]

Figure 8(b) shows the electronic population of the initial state $|B_A^- H_A\rangle$ as a function of time at different temperatures. Temperature effects are not dramatic, as expected, since most of the vibronic activity is associated with high frequency vibrations. Increasing the temperature from 10 K to 77 K results in a very small decrease of the decay rate. This

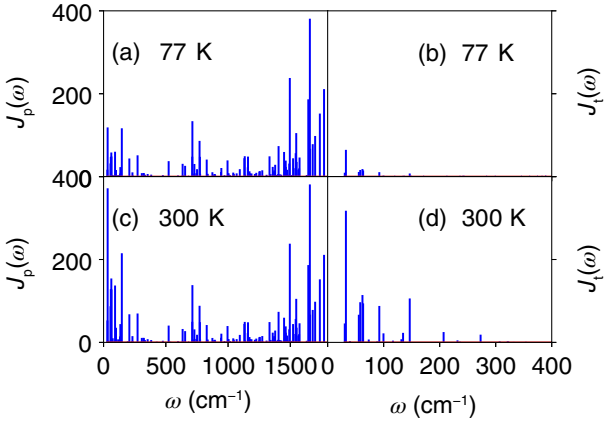

FIGURE 7 Effective site spectral densities $J_p(\omega)$ and $J_t(\omega)$ describing the coupling of the physical and tilde bosonic DoFs with the electronic subsystem at different temperatures. (a,b) 77 K, (c,d) 300 K

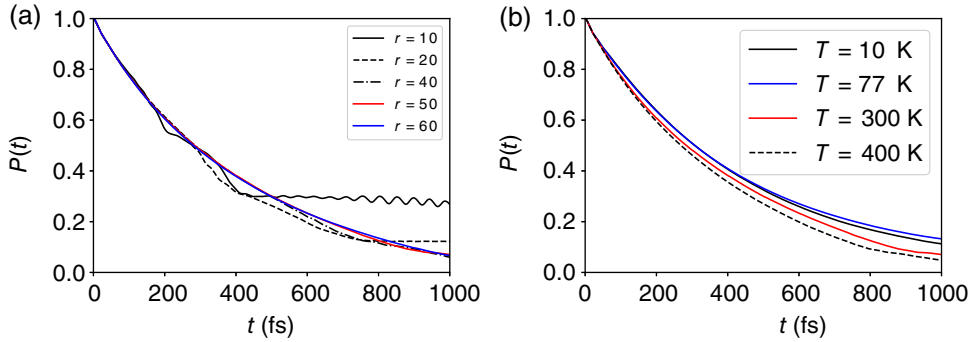

FIGURE 8 (a) Electronic population of the initially populated state $|B_A^{\sim}H_A\rangle$ (a) for different values of the TT compression ranks; (b) for different values of the temperature, TT ranks are set to 50

effect cannot be described in the framework of the classical ET theory and is very likely due to the highly quantized nature of the vibrational density of states at very low temperatures. A modest increase in the population decay rate upon increasing T from 77 K to 298 K is observed. This effect can be attributed to the increased number of accessible vibronic states. The overall behavior is similar to what is found in other ET processes where large vibronic couplings are associated to highly quantized modes.[97–99]

5 | OPEN SYSTEMS AND HIERARCHICAL EQUATION OF MOTION IN TWIN-SPACE TENSOR-TRAIN FORMALISM

5.1 | Theoretical formulation

As discussed in the preceding sections the twin-space formulation of the Liouville–von Neuman equation enables the development of the TFD Schrödinger equation. Furthermore, using this formalism it is possible to define a reduced state vector analogous to the familiar reduced density matrix. This was first discussed by Arimitsu and Umezawa[44] using projection operator techniques and leads to a set of equations which share the same formal structure as the standard reduced density matrix approaches, but make explicit use of tilde operators. We have recently demonstrated that this procedure can be used to derive an equation of motion for the reduced density matrix based on the hierarchical solver technique developed by Tanimura and Kubo.[100,101]

Here we briefly sketch the main steps of the derivation and refer the reader to the original article[12] for further details. Let us consider a system described by a Hamiltonian operator

$$H = H_A + H_B + V = H_0 + V \tag{69}$$

where A is the subsystem of interest, B is the "bath," that is, the irrelevant subsystem, V is their coupling, and $H_0 = H_A + H_B$. In twin-space formulation the Liouville super-operator is thus given by

$$\hat{H} = H_A + H_B + V - \tilde{H}_A - \tilde{H}_B - \tilde{V} = \hat{H}_A + \hat{H}_B + \hat{V} = \hat{H}_0 + \hat{V} \tag{70}$$

where $\hat{H}_A = H_A - \tilde{H}_A$ and so on.

The HEOM theory by Kubo and Tanimura[100] is certainly one of the most important theoretical developments for the study of open systems. It was originally formulated as a methodology to describe a system interacting with a non-Markovian Gaussian environment, and has later been extended to treat other types of system–bath interactions.[100,102] In its current formulation it has been applied to study the dynamics of a large variety of chemico-physical processes including energy and electron transfer[83,87,103–105] as well as heat transport[106] and electron transport.[7] The reader can refer to the recent work by Tanimura[4] for a more detailed analysis of the HEOM methodology.

A fundamental assumption of HEOM theory is that the system–bath interaction can be factorized as

$$V = \sum_k S_k Q_k \tag{71}$$

where S_k and Q_k are system and bath operators respectively. Furthermore, the bath operators are described as a linear combination of position operators q_j of harmonic oscillators

$$Q_k = \sum_j g_{kj} q_j. \tag{72}$$

The coupling super-operator is thus given by

$$\hat{V} = \sum_k S_k Q_k - \sum_k \tilde{S}_k \tilde{Q}_k. \tag{73}$$

Under this conditions it is possible to demonstrate that[107,108]

$$|\rho_A(t)\rangle_I = T_+ \exp\left(-\int_0^t \hat{K}_I^{(2)}(s)ds\right)|\rho_A(0)\rangle_I \tag{74}$$

where $|\rho_A(t)\rangle_I$ is the reduced density matrix of subsystem A obtained by tracing over all the possible states of the "irrelevant" subsystem B, and

$$\hat{K}_I^{(2)}(s) = \int_0^s d\tau \langle \hat{V}(s)\hat{V}(\tau)\rangle, \tag{75}$$

$\hat{V}(t) = e^{i\hat{H}_0 t}\hat{V}e^{-i\hat{H}_0 t}$ being the coupling between subsystems A and B in the interaction picture.

Differentiating Equation (74) one obtains[109]

$$\frac{\partial}{\partial t}|\rho_A(t)\rangle_I = -T_+ \int_0^t d\tau \langle \hat{V}(t)\hat{V}(\tau)\rangle \exp\left(-\int_0^t \hat{K}_I^{(2)}(s)ds\right)|\rho_A(0)\rangle_I. \tag{76}$$

It is fundamental to note that the variable τ in the integral above ranges over all times, so that, for $\tau < s$ the time ordering operator mixes $\hat{V}(\tau)$ with all the terms of the expansion of the exponential operator $\exp\left(-\int_0^t \hat{K}_I^{(2)}(s)ds\right)$, making it impossible to obtain an explicit equation for $|\rho_A(t)\rangle_I$. The HEOM method provides a way to disentangle the above equation in the special case of a Gaussian bath.

Indeed, it is possible to demonstrate that after some easy manipulations the second order cumulant can be written as (see Ref. 12)

$$\hat{K}_I^{(2)}(t) = \sum_k \left[S_k(t) - \tilde{S}_k(t)\right]\left\{\int_0^t dt_1 \langle Q_k(t)Q_k(t_1)\rangle S_k(t_1) - \int_0^t dt_1 \langle Q_k(t_1)Q_k(t)\rangle \tilde{S}_k(t_1)\right\}, \tag{77}$$

where $S(t), \tilde{S}(t)$, and $Q(t)$ are operators in the interaction picture. In the limit of a continuous distribution of bath modes the correlation function $\langle Q_k(t_1)Q_k(t)\rangle$ can be written as

$$\langle Q_k(t_1)Q_k(t)\rangle = \frac{1}{\pi}\int_0^\infty d\omega J_k(\omega)[\coth(\beta\omega/2)\cos(\omega(t_1 - t)) + i\sin(\omega(t_1 - t))] \tag{78}$$

where $J_k(\omega)$ is the k-th bath spectral density. Furthermore, if Equation (78) can be represented as series of the form

$$\langle Q_k(t_1)Q_k(t)\rangle = \sum_{j=1}^\infty c_{kj} e^{-\gamma_{kj}|t - t_1|} \tag{79}$$

where c_{kj} and γ_{kj} are complex coefficients, the second order cumulant reduces to

$$\hat{K}_I^{(2)}(t) = \sum_{kj} \hat{S}_k(t) \int_0^t d\tau e^{-\gamma_{kj}|t-\tau|} \hat{R}_{kj}(\tau) \tag{80}$$

in which we have introduced the super-operators

$$\hat{S}_k(t) = \left[S_k(t) - \tilde{S}_k(t)\right] \tag{81}$$

$$\hat{R}_{kj}(t) = c_{kj} S_k(t) - c_{kj}^* \tilde{S}_k(t). \tag{82}$$

As a last step of our derivation we define a set of auxiliary state vectors[100,110]

$$|\rho_A^{\mathbf{m}}(t)\rangle = T_+ \prod_{kj} \left(m_{kj}! |c_{kj}|^{m_{kj}}\right)^{-1/2} \left(i \int_0^t dt_1 e^{-\gamma_k|t-t_1|} \hat{R}_{kj}(\tau)\right)^{m_{kj}} \exp\left(-\int_0^t \hat{K}_I^{(2)}(s) ds\right) |\rho_A(0)\rangle_I \tag{83}$$

where $\mathbf{m} = \{m_{kj}\}$ is a set of non-negative integers. Here, the index k labels the number of independent bath spectral densities $J_k(\omega)$, and the index j labels the number of terms in the expansion of Equation (79). It is readily verified that the vector $|\rho_A(t)\rangle_I$, describing the physical state of our system, corresponds to the auxiliary state vector having all indices $m_{kj} = 0$, that is, $|\rho_A(t)\rangle_I = |\rho_A^{\mathbf{0}}(t)\rangle$. The above definition takes into account the scaling factors originally proposed by Shi and coworkers which improves the numerical stability of the final system of equations.[110] HEOM are readily derived upon repeated differentiation of the $|\rho^{\mathbf{m}}\rangle$ with respect to time. Moving to the Schrödinger representation the set of equations

$$\frac{\partial}{\partial t}|\rho_A^{\mathbf{m}}\rangle = -\left(i\hat{H}_A + \sum_{kj} m_{kj}\gamma_{kj}\right)|\rho_A^{\mathbf{m}}\rangle - i\sum_{kj}\sqrt{m_{kj}/|c_{kj}|}\left(c_{kj}S_k - c_{kj}^*\tilde{S}_k\right)|\rho_A^{\mathbf{m}-1_{kj}}\rangle$$

$$-i\sum_{kj}\sqrt{(m_{kj}+1)|c_{kj}|}\left(S_k - \tilde{S}_k\right)|\rho_A^{\mathbf{m}+1_{kj}}\rangle \tag{84}$$

is obtained, where $\mathbf{m} \pm 1_{kj} = (m_{10}, ..., m_{kj} \pm 1, ...)$, and the explicit time dependence of the auxiliary vectors has been dropped. The price to pay for disentangling the time ordering operation of Equation (74) is that HEOM constitutes an infinite set of first-order ordinary differential equations. Fortunately, using the hierarchy it is possible to devise very efficient truncation schemes which enable obtaining highly accurate results with a finite system. The reader is referred to the original articles for the derivation of an optimal truncation scheme.[100,111] In the above derivation we have not considered low-temperature corrections which can be included straightforwardly from a direct application of the original approach suggested by Ishizaki and Tanimura.[111]

To further simplify the structure of the HEOMs we follow Tanimura[102] and introduce a set of vectors $|\mathbf{m}\rangle = |m_{10}m_{11}...m_{1K}m_{20}...m_{MK}\rangle$, and their corresponding boson-like creation-annihilation operators b_{kj}^+, b_{kj}^-

$$b_{kj}^+|\mathbf{m}\rangle = \sqrt{(m_{kj}+1)}|\mathbf{m}+1_{kj}\rangle \quad b_{kj}^-|\mathbf{m}\rangle = \sqrt{m_{kj}}|\mathbf{m}-1_{kj}\rangle \quad b_{kj}^+ b_{kj}^-|\mathbf{m}\rangle = m_{kj}|\mathbf{m}\rangle \tag{85}$$

and the auxiliary density vector

$$|\eta\rangle = \sum_{\mathbf{m}} |\rho_A^{\mathbf{m}}\rangle |\mathbf{m}\rangle \tag{86}$$

and rewrite the hierarchical equations of motion in the compact form

$$\frac{\partial}{\partial t}|\eta\rangle = \left(-i\hat{H}_A - \sum_{kj}\gamma_{kj}b_{kj}^{+}b_{kj}^{-} - i\sum_{kj}\sqrt{|c_{kj}|}\left(S_k - \tilde{S}_k\right)b_{kj}^{-} - i\sum_{kj}\frac{\left(c_{kj}S_k - c_{kj}^{*}\tilde{S}_k\right)}{\sqrt{|c_{kj}|}}b_{kj}^{+}\right)|\eta\rangle, \tag{87}$$

with the initial condition given by $|\eta(0)\rangle = |\rho_A(0)\rangle|\mathbf{0}\rangle$.

5.2 | Tensor-train representation of the auxiliary reduced density vector

Tensor train representation can be applied to the density vector $|\eta\rangle$ in a manner that is similar to that used for the treatment of the thermal Schrödinger equation. If d is the dimensionality of the original Hilbert space of our system, that is the number of DoFs of the H_A Hamiltonian operator, and if the dissipative environment is described using M uncorrelated spectral densities $J_k(\omega)$ each expanded into K Matstubara terms, the vector $|\eta(t)\rangle$ of Equation (86) can be considered as a tensor with $N = 2d + KM$ indices. Therefore, one possible way to represent $|\eta(t)\rangle$ in TT format is to employ a product of $2d + MK$ low rank matrices. For sake of simplicity, in the following only one Matsubara term is considered for each spectral density, $K = 1$. The generalization to $K > 1$ requires a slightly more involved notation. If we label with $\mu_k(m_k)$ the TT core matrices associated with the ith spectral density, and with $\rho_{2f-1}(i_f)$, $(\rho_{2f}(\tilde{j}_f))$ the TT core matrices associated with the fth physical (tilde) DoFs, $|\eta(t)\rangle$ can be written in TT form as

$$|\eta(t)\rangle = \sum_{\substack{m_1,m_2,\ldots \\ i_1\tilde{j}_1\ldots i_d,\tilde{j}_d}} \mu_1(m_1)\ldots\mu_M(m_M)\rho_1(i_1)\rho_2(\tilde{j}_1)\ldots\rho_{2d-1}(i_d)\rho_{2d}(\tilde{j}_d)\,|\,m_1\ldots m_K; i_1\tilde{j}_1\ldots i_d\tilde{j}_d\rangle. \tag{88}$$

In the above expression only the component with $\{m_k = 0,\ k = 1,\ ...,\ M\}$ is required for the computation of physical observables, that is

$$|\rho_A(t)\rangle = \mu_1(0)\ldots\mu_M(0)\sum_{i_1\tilde{j}_1\ldots i_d,\tilde{j}_d}\rho_1(i_1)\rho_2(\tilde{j}_1)\ldots\rho_{2d-1}(i_d)\rho_{2d}(\tilde{j}_d)\,|\,i_1\tilde{j}_1\ldots i_d\tilde{j}_d\rangle. \tag{89}$$

The alternation of the indices $i_k, \tilde{j}_k$ provides a very convenient scheme for the computation of expectation values of observables. Indeed, the identity vector can easily be written as a direct product

$$|I\rangle = \sum_{i_1}|i_1\rangle|\tilde{i}_1\rangle \otimes \sum_{i_2}|i_2\rangle|\tilde{i}_2\rangle \otimes \ldots \otimes \sum_{i_d}|i_d\rangle|\tilde{i}_d\rangle \tag{90}$$

which can be directly translated into the TT format, since, as already mentioned in Section 3.1, the Kronecker product can be considered a TT in which all the ranks of the cores are 1. From the above expression it is immediate to derive TT representations of the vectors corresponding to observables using Equation (3). We notice that a different order of the indices would make the summations not separable increasing the overall computational cost. Finally, the use of tilde operators allows to easily perform grouping of variables that are strongly correlated.[13]

5.3 | Application of twin-space TT-HEOM to model systems

The methodology described above has already been successfully applied to the study of spin-boson and exciton-polaron systems. Here we briefly report on an illustrative application to a charge transfer problem between two identical molecular sites. Both sites are linearly coupled to a set of seven nuclear vibrations. The parameters of the vibronic model are reported elsewhere[12] and have been used to describe the charge-transfer (CT) process in a pentacene dimer.[112]

In Figure 9(a) the population dynamics of the two site system is reported for two different values of the bath reorganization energy $\lambda = 300$ and 90 cm^{-1}. In both cases the characteristic bath frequency is $\gamma = 53$ cm^{-1}. Due to the complexity of the model and to the large number of vibronically active DoFs it is not easy to disentangle the different contributions to the population dynamics. The initial fast decay of the populations is very likely due to pure excitonic couplings[113] while the small oscillations with periods of about 20 fs, clearly evident at longer times, are caused by the vibronic activity of several high frequency modes. For $\lambda = 90$ cm^{-1} the CT dynamics is underdamped while an overall overdamped behavior can be observed for $\lambda = 300$ cm^{-1}.

Finally, the convergence properties of the numerical methodology are illustrated in Figure 9(b) where the populations of the two states of the dimer model as a function of time for different values of the TT compression ranks are compared. Considering the relatively small number of DoFs the ranks necessary to reach a converged dynamics are considerably large. Figure 9(c) also shows the norm of the state vector as a function of time. As can be readily seen for very small ranks the norm drastically decreases, by about 20%, after a very short time and even for very large ranks ($r = 115$) there is a 1% loss after 800 fs. This behavior can be traced back to the combination of the reduced Liouville equation with the TDVP solver.[114,115] Indeed, this methodology preserves the norm $\langle\Psi|\,\Psi\rangle$ and the mean value $\langle\Psi|\,X|\,\Psi\rangle$ during the evolution governed by Equation (87). Both quantities however have no direct physical meaning. In our formalism the true norm to be preserved during the evolution is $\langle 1|\rho_A^{\mathbf{0}}(t)\rangle = \mathrm{tr}\rho_A^{\mathbf{0}}(t) = 1$. As can be expected this problem introduces artifacts which can be alleviated by increasing the ranks of the TT cores. However, this easily becomes a limiting factor since the required TT storage scales quadratically with the TT ranks. Very recently Shi et al.,[116] following the original idea of Heller[115] have suggested to correct the norm conservation problem by adding a constraint via an additional Lagrange multiplier.

6 | FURTHER DEVELOPMENTS

The TFD-TT framework offers ready-to-use methodology for the simulation of quantum dynamics of a broad class of electron-vibrational systems with many DoFs at finite temperature. The methodology can be applied to various polyatomic species and molecular aggregates of practical interest. Apart from that, two other directions should be highlighted. (a) TFD-TT simulations, if converged, provide numerically accurate quantum dynamics. Such simulations can therefore be employed for benchmarking evolutions of selected quantum systems and testing different approximate quantum/quasiclassical/semiclassical simulation protocols. (b) The TFD-TT methodology is valid, without any alterations, for time-dependent Hamiltonians. It is thus tempting to apply it to driven systems, to problems of quantum control, and to simulations of nonlinear femtosecond spectroscopic signals. For example, Begušić and Vaníček have recently combined TFD machinery with the single-trajectory semiclassical thawed Gaussian approximation, which allowed them to simulate third-order response functions and spectroscopic signals on the fly.[117]

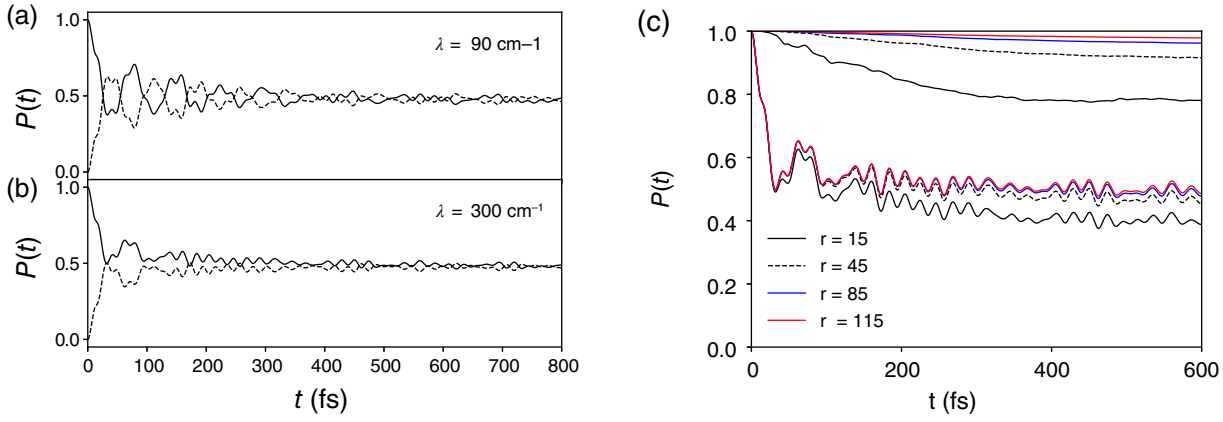

FIGURE 9 Population dynamics of a homodimer with 14 nuclear vibrations. Bath reorganization energies are (a) 90 cm^{-1}; (b) 300 cm^{-1}. (c) Convergence of the norm for different TT truncation ranks as indicated in the legend. Converged results are obtained with TT ranks 115. The hierarchy level is truncated at $m = 10$ on each bath

The TFD-TT methodology is not only an efficient suite of algorithms and codes for the simulation of quantum dynamics. This methodology, in which temperature is incorporated into the Hamiltonian, offers a new paradigm of the description of molecular species. Any electron-vibrational system specified by the Hamiltonian H, the density matrix $\rho(t)$, and the initial thermal vibrational distribution $\rho(0)$ is equivalently described by the thermal Hamiltonian $\bar{H}_\theta$ with twice higher number of vibrational modes possessing temperature-dependent electron-vibrational couplings, but characterized by the thermal wave function $|\psi_\theta(t)\rangle$ prepared initially in the global electron-vibrational vacuum state $|\psi_\theta(0)\rangle = |0_A\rangle\,|0_B\tilde{0}_B\rangle$. Putting differently, the TFD methodology maps the Schrödinger equation driven by the Hamiltonian H at zero temperature to the TFD Schrödinger equation driven by the thermal Hamiltonian $\bar{H}_\theta$ at finite temperature. This analogy is useful for the development of TFD picture of various aspects of quantum dynamics of molecular systems. For example, one can study semiclassical evolution generated by the TFD-version of the van Vleck–Gutzwiller and Herman–Kluk propagators, or introduce temperature-dependent Franck–Condon and Huang–Rhys factors for electron-vibrational transitions. Note also that quantum dynamics driven by the TFD Schrödinger equation can directly be simulated by the MCTDH methods. This observation uncovers deep interconnection between the MCTDH and TFD-TT methods, as well as calls for their application to the same systems for comparing numerical efficiency of the two methods.

As has been noted above, the TFD-TT methodology can readily be generalized to a broader class of Hamiltonians in which site energies ε_n, electronic couplings V_{nm}, and electron-vibrational coupling constants g_{kn} are polynomials in vibrational creation-annihilation operators. For example, a conical intersection between the electronic states n and m driven by the vibrational coupling mode j corresponds to $V_{nm} \sim a_j + a_j^\dagger$. Hence finite-temperature quantum dynamics of a larger number of important for applications molecular systems can be scrutinized by the TFD-TT machinery. The TFD-TT approach can also be extended to rovibrational systems, where vibrational subsystem should be considered as fast, while rotational subsystem should be thermalized and treated as slow.

The present methodology is based on the Born–Oppenheimer approximation of Equation (20), which implies that the electron-vibrational system is initially prepared in the ground state of the electronic subsystem with thermal distribution over the DoFs of the vibrational subsystem. The extension beyond the Born–Oppenheimer approximation, which is valid for initially correlated thermal electron-vibrational systems, has been theoretically developed in Ref. 51 and needs to be tested in explicit simulations.

Finally, it looks promising to apply the TFD-TT methodology to study inter-molecular and intra-molecular vibrational energy redistribution and transfer. These problems, which are conceptually rooted into venerable Fermi–Pasta–Ulam model, require accurate simulation of quantum dynamics of nonlinearly coupled oscillators in the electronic ground state. Very recently, the first step in this direction was made in Ref. 118, where the TT methodology was applied to investigate energy transfer between two localized vibrational modes nonlinearly (via Fermi-resonance) coupled to the chain of harmonic oscillators. Since high-frequency modes were considered only, thermal effects were insignificant in that study. The inclusion of low-frequency modes into similar models and simulation of the ensuing nonlinear multiscale quantum dynamics via TFD-TT methods is currently under way.

As for the twin-space TT-HEOM formulation the field of application can be potentially very similar to that of the TFD-TT approach.

7 | CONCLUSION

In this work, we have presented a comprehensive overview of recent theoretical development which enables accurate finite-temperature quantum dynamical simulations of systems with multiple electronic and nuclear DoFs. The approach is based on TFD theory and TT decomposition. TFD describes temperature effects by the coupling of the system to a fictitious bosonic bath, so that the number of nuclear DoFs is doubled. In a basis-set representation, the time-dependent TFD wave function is an array of the dimension $M \times d^2$, where M and d are the number of electronic and vibrational basis DoFs respectively. The density matrix describing the same problem has the dimension of $M^2 \times d^2$. The TFD wave function offers, therefore, a more compact way of information storage in comparison with the density matrix, notably for systems with multiple electronic states. Furthermore, high-frequency modes need not be coupled to the fictitious bosonic bath. This leads to additional reduction of the active space and computational savings. A new time-dependent TFD Schrödinger equation has been proposed and its numerical solution via TT/MPS representation of the

vibronic wave function has been discussed in detail. Our approach to the application of TFD has provided a new view of quantum dynamics at finite temperature, by introducing temperature-renormalized electron-vibrational couplings and spectral densities. This picture shows explicitly which DoFs are thermalized, and which are not.

The use of TT decomposition enables to handle a large number of variables: the storage of order N tensors in TT/MPS format scales linearly with N. The results of our numerical simulations of energy and charge transfer processes clearly show that the methodology is very accurate and robust, and it can be applied to problems with many DoFs at any temperature. The present approach is based on a basis set representation of the wave function and can in principle be applied to realistic chemical dynamics problems using computed potential energy surfaces.

In standard wave function methodologies, finite temperature effects are taken into account by averaging the quantity of interest over different initial conditions. Therefore, the distribution of initial conditions must be sampled via Monte Carlo methods, and for each initial state a separate dynamical problem must be solved. Both these aspects limit the applications of such methods to large systems at room temperature. Here we have shown that using TFD theory it is possible to describe finite temperature effects without the need to solve a large number of independent dynamical problems with different initial conditions. The increased computational cost, due to the doubled number of nuclear DoFs, can be kept under control by using a TT/MPS representation of the wave function, which is very accurate for the cases discussed in this article.

TT have revealed to be a very promising approximation of the wave function of vibronic systems, allowing to describe molecular processes with multiple coupled electronic states. The very simple structure of the tensor network makes the TT approximation suitable for the development of automatic procedures to optimize the sequence of indices which provide an optimal entanglement growth, although this latter point is still a subject of active research.

Finally, we have shown that by employing the twin formulation of quantum statistical mechanics it is possible to extend the use of numerical methods suitable for wave-packet propagation directly to the study of reduced density matrix evolution in open systems. The proposed approach is based on the twin-space formulation of quantum statistical mechanics and introduces a significant benefit to the actual numerical calculations of expectation values of dynamical operators of system variables. A key advantage of the mathematical description of HEOM reported here is that it allows to fully exploit the TT formalism in the double Hilbert space.

ACKNOWLEDGMENTS

This project has received funding from the European Union's Horizon 2020 research and innovation programmer under grant agreement No. 826013. The financial support from The University of Torino through the local research funding Grant No. BORR-RILO-19-01 is acknowledged. M.F.G. acknowledges support of Hangzhou Dianzi University through the startup funding. R.B. acknowledges the HP10CTVK2K and HP10CU4N9A CINECA awards under the ISCRA initiative, for the availability of high performance computing resources and support.

CONFLICT OF INTEREST

The authors have declared no conflicts of interest for this article.

AUTHOR CONTRIBUTIONS

Raffaele Borrelli: Data curation; formal analysis; methodology; resources; software; validation; writing-original draft.
Maxim Gelin: Formal analysis; investigation; methodology; software; validation.

DATA AVAILABILITY STATEMENT

Data sharing is not applicable to this article as no new data were created or analyzed in this study.

ORCID

Raffaele Borrelli https://orcid.org/0000-0002-0060-4520
Maxim F. Gelin https://orcid.org/0000-0003-3092-3343

RELATED WIREs ARTICLE

Theoretical study of excitation energy transfer and nonlinear spectroscopy of photosynthetic light-harvesting complexes using the nonperturbative reduced dynamics method

REFERENCES

1. Domcke W, Stock G. Theory of ultrafast nonadiabatic excited-state processes and their spectroscopic detection in real time. *Adv Chem Phys*. 1997;*100*:1–169.
2. Wang H, Thoss M. Multilayer formulation of the multiconfiguration time-dependent Hartree theory. *J Chem Phys*. 2003;*119*(3):1289–99.
3. Oseledets I, Tyrtyshnikov E. Breaking the curse of dimensionality, or how to use SVD in many dimensions. *SIAM J Sci Comput*. 2009;*31*(5):3744–59.
4. Tanimura Y. Numerically "exact" approach to open quantum dynamics: the hierarchical equations of motion (HEOM). *J Chem Phys*. 2020;*153*(2):020901.
5. Kreisbeck C, Kramer T, Rodríguez M, Hein B. High-performance solution of hierarchical equations of motion for studying energy transfer in light-harvesting complexes. *J Chem Theory Comput*. 2011;*7*(7):2166–74.
6. Yao Y, Sun K-W, Luo Z, Ma H. Full quantum dynamics simulation of a realistic molecular system using the adaptive time-dependent density matrix renormalization group method. *J Phys Chem Lett*. 2018;*9*(2):413–9.
7. Thoss M, Evers F. Theory of quantum transport in molecular junctions. *J Chem Phys*. 2018;*148*(3):030901.
8. Li W, Ren J, Shuai Z. Finite-temperature TD-DMRG for the carrier mobility of organic semiconductors. *J Phys Chem Lett*. 2020;*11*(13):4930–6.
9. Borrelli R, Gelin MF. Quantum electron-vibrational dynamics at finite temperature: thermo field dynamics approach. *J Chem Phys*. 2016;*145*(22):224101.
10. Borrelli R, Gelin MF. Simulation of quantum dynamics of Excitonic Systems at Finite Temperature: an efficient method based on thermo field dynamics. *Sci Rep*. 2017;*7*(1):9127.
11. Borrelli R. Theoretical study of charge-transfer processes at finite temperature using a novel thermal Schrödinger equation. *Chem Phys*. 2018;*515*:236–41.
12. Borrelli R. Density matrix dynamics in twin-formulation: an efficient methodology based on tensor-train representation of reduced equations of motion. *J Chem Phys*. 2019;*150*(23):234102.
13. Beck MH, Jackle A, Worth GA, Meyer HD. The multiconfiguration time-dependent Hartree (MCTDH) method: a highly efficient algorithm for propagating wavepackets. *Phys Rep*. 2000;*324*(1):1–105.
14. Burghardt I, Giri K, Worth GA. Multimode quantum dynamics using Gaussian wavepackets: the Gaussian-based multiconfiguration time-dependent Hartree (G-MCTDH) method applied to the absorption spectrum of pyrazine. *J Chem Phys*. 2008;*129*(17):174104.
15. Wang H. Multilayer multiconfiguration time-dependent Hartree theory. *J Phys Chem A*. 2015;*119*(29):7951–65.
16. White SR, Adrian E. Feiguin real-time evolution using the density matrix renormalization group. *Phys Rev Lett*. 2004;*93*(7):076401.
17. Wang H, Song X, Chandler D, Miller WH. Semiclassical study of electronically nonadiabatic dynamics in the condensed-phase: spin-boson problem with Debye spectral density. *J Chem Phys*. 1999;*110*(10):4828–40.
18. Kondov I, Thoss M, Wang H. Theoretical study of ultrafast heterogeneous electron transfer reactions at dye-semiconductor interfaces: Coumarin 343 at titanium oxide. *J Phys Chem A*. 2006;*110*(4):1364–74.
19. Borrelli R, Di Donato M, Peluso A. Quantum dynamics of electron transfer from bacteriochlorophyll to pheophytin in bacterial reaction centers. *J Chem Theory Comput*. 2007;*3*(3):673–80.
20. Wang H, Thoss M. Theoretical study of ultrafast photoinduced electron transfer processes in mixed-valence systems. *J Phys Chem A*. 2003;*107*(13):2126–36.
21. Umezawa H, Matsumoto H, Tachiki M. *Thermofield dynamics and condenced states*. Amsterdam: North-Holland Publishing Company; 1982.
22. Takahashi Y, Umezawa H. Thermo field dynamics. *Int J Mod Phys B*. 1996;*10*:1755–805.
23. Kosov DS. Nonequilibrium Fock space for the electron transport problem. *J Chem Phys*. 2009;*131*(17):171102.
24. Dzhioev AA, Kosov DS. Nonequilibrium configuration interaction method for transport in correlated quantum systems. *J Phys A: Math Theor*. 2014;*47*(9):095002.
25. Harsha G, Henderson TM, Scuseria GE. Thermofield theory for finite-temperature quantum chemistry. *J Chem Phys*. 2019;*150*(15):154109.
26. Harsha G, Henderson TM, Scuseria GE. Thermofield theory for finite-temperature coupled cluster. *J Chem Theory Comput*. 2019;*15*(11):6127–36.
27. Ritschel G, Suess D, Möbius S, Strunz WT, Eisfeld A. Non-Markovian quantum state diffusion for temperature-dependent linear spectra of light harvesting aggregates. *J Chem Phys*. 2015;*142*(3):034115.
28. Reddy CS, Prasad MD. Finite temperature vibronic spectra of harmonic surfaces: a time-dependent coupled cluster approach. *Mol Phys*. 2015;*113*(19–20):3023–30.
29. Greene SM, Batista VS. Tensor-train split-operator fourier transform (TT-SOFT) method: multidimensional nonadiabatic quantum dynamics. *J Chem Theory Comput*. 2017;*13*(9):4034–42.
30. Ren J, Shuai Z, Chan GK-L. Time-dependent density matrix renormalization group algorithms for nearly exact absorption and fluorescence spectra of molecular aggregates at both zero and finite temperature. *J Chem Theory Comput*. 2018;*14*(10):5027–39.
31. Jiang T, Li W, Ren J, Shuai Z. Finite temperature dynamical density matrix renormalization group for spectroscopy in frequency domain. *J Phys Chem Lett*. 2020;*11*(10):3761–8.

32. Xie X, Liu Y, Yao Y, Schollwöck U, Liu C, Ma H. Time-dependent density matrix renormalization group quantum dynamics for realistic chemical systems. *J Chem Phys*. 2019;*151*(22):224101.
33. Begušić T, Vaníček J. On-the-fly ab initio semiclassical evaluation of vibronic spectra at finite temperature. *J Chem Phys*. 2020;*153*(2):024105.
34. Orús R. A practical introduction to tensor networks: matrix product states and projected entangled pair states. *Ann Phys Rehabil Med*. 2014;*349*:117–58.
35. Oseledets I. Tensor-train decomposition. *SIAM J Sci Comput*. 2011;*33*(5):2295–317.
36. Lubich C, Oseledets I, Vandereycken B. Time integration of tensor trains. *SIAM J Numer Anal*. 2015;*53*(2):917–41.
37. Tanimura Y, Kubo R. Time evolution of a quantum system in contact with a nearly Gaussian-Markoffian noise bath. *J Phys Soc Jpn*. 1989;*58*(1):101–14.
38. Arimitsu T, Umezawa H. A general formulation of nonequilibrium thermo field dynamics. *Prog Theor Phys*. 1985;*74*(2):429–32.
39. Suzuki M. Density matrix formalism, double-space and thermo field dynamics in non-equilibrium dissipative systems. *Int J Mod Phys B*. 1991;*05*(11):1821–42.
40. Suzuki M. Thermo field dynamics in equilibrium and non-equilibrium interacting quantum systems. *J Phys Soc Jpn*. 1985;*54*(12):4483–5.
41. Schmutz M. Real-time green's functions in many body problems. *Z Phys B*. 1978;*30*(1):97–106.
42. Fano U. Description of states in quantum mechanics by density matrix and operator techniques. *Rev Mod Phys*. 1957;*29*(1):74–93.
43. Mukamel S. *Principles of nonlinear optical spectroscopy*. New York: Oxford University Press; 1995.
44. Arimitsu T, Umezawa H. Non-equilibrium thermo field dynamics. *Prog Theor Phys*. 1987;*77*(1):32–52.
45. Suzuki M. Quantum analysis, nonequilibrium density matrix and entropy operator. *Int J Mod Phys B*. 1996;*10*:1637–47.
46. Chernyak V, Mukamel S. Collective coordinates for nuclear spectral densities in energy transfer and femtosecond spectroscopy of molecular aggregates. *J Chem Phys*. 1996;*105*(11):4565–83.
47. Mukamel S, Abramavicius D. Many-body approaches for simulating coherent nonlinear spectroscopies of electronic and vibrational excitons. *Chem Rev*. 2004;*104*(4):2073–98.
48. Huynh TD, Sun K-W, Gelin M, Zhao Y. Polaron dynamics in two-dimensional photon-echo spectroscopy of molecular rings. *J Chem Phys*. 2013;*139*(10):104103.
49. Köppel H, Domcke W, Cederbaum LS. Multimode molecular dynamics beyond the born-Oppenheimer approximation. *Advances in chemical physics*. Volume 57. Hoboken, NJ: John Wiley & Sons, Inc; 1984. p. 59–246.
50. Bunker PR, Jensen P. *Molecular symmetry and spectroscopy*. Ottawa: NRC Research Press; 1998.
51. Gelin MF, Borrelli R. Thermal Schrödinger equation: efficient tool for simulation of many-body quantum dynamics at finite temperature. *Ann Phys*. 2017;*529*(12):1700200.
52. Crawford JA. An alternative method of quantization: the existence of classical fields. *Nuovo Cim*. 1958;*10*(4):698–713.
53. Barnett SM, Knight PL. Thermofield analysis of squeezing and statistical mixtures in quantum optics. *J Opt Soc Am B*. 1985;*2*(3):467.
54. Matzkies F, Manthe U. A multi-configurational time-dependent Hartree approach to the direct calculation of thermal rate constants. *J Chem Phys*. 1997;*106*(7):2646–53.
55. Matzkies F, Manthe U. Accurate reaction rate calculations including internal and rotational motion: a statistical multi-configurational time-dependent Hartree approach. *J Chem Phys*. 1999;*110*(1):88–96.
56. Wang H, Thoss M. Quantum-mechanical evaluation of the Boltzmann operator in correlation functions for large molecular systems: a multilayer multiconfiguration time-dependent Hartree approach. *J Chem Phys*. 2006;*124*(3):034114.
57. Louisell WH. *Quantum statistical properties of radiation*. New York, NY: Wiley; 1973.
58. Bogoljubov NN. On a new method in the theory of superconductivity. *Nuovo Cim*. 1958;*7*(6):794–805.
59. Ojima I. Gauge fields at finite temperatures— "thermo field dynamics" and the KMS condition and their extension to gauge theories. *Ann Phys Rehabil Med*. 1981;*137*(1):1–32.
60. Caldeira AO, Leggett AJ. Quantum tunnelling in a dissipative system. *Ann Phys*. 1983;*149*(2):374–456.
61. Barnett SM, Knight PL. Comment on "obtainment of thermal noise from a pure quantum state". *Phys Rev A*. 1988;*38*(3):1657–8.
62. Zhao Y, Yokojima S, Chen GH. Reduced density matrix and combined dynamics of electrons and nuclei. *J Chem Phys*. 2000;*113*(10):4016–27.
63. Marcus RA. Nonadiabatic processes involving quantum-like and classical-like coordinates with applications to nonadiabatic electron transfers. *J Chem Phys*. 1984;*81*(10):4494–500.
64. Borrelli R, Capobianco A, Landi A, Peluso A. Vibronic couplings and coherent electron transfer in bridged systems. *Phys Chem Chem Phys*. 2015;*17*(46):30937–45.
65. Holtz S, Rohwedder T, Schneider R. On manifolds of tensors of fixed TT-rank. *Numer Math*. 2011;*120*(4):701–31.
66. Paeckel S, Köhler T, Swoboda A, Manmana SR, Schollwöck U, Hubig C. Time-evolution methods for matrix-product states. *Ann Phys Rehabil Med*. 2019;*411*:167998.
67. Sergey VD. A tensor decomposition algorithm for large ODEs with conservation Laws. *Comput Methods Appl Math*. 2019;*19*(1):23–38.
68. Vidal G. Efficient classical simulation of slightly entangled quantum computations. *Phys Rev Lett*. 2003;*91*(14):147902.
69. Verstraete F, García-Ripoll JJ, Cirac JI. Matrix product density operators: simulation of finite-temperature and dissipative systems. *Phys Rev Lett*. 2004;*93*(20):207204.
70. Wall ML, Carr LD. Out-of-equilibrium dynamics with matrix product states. *New J Phys*. 2012;*14*(12):125015.

71. Jutho Haegeman J, Cirac I, Osborne TJ, Pižorn I, Verschelde H, Verstraete F. Time-dependent Variational principle for quantum lattices. *Phys Rev Lett*. 2011;*107*(7):070601.
72. Haegeman J, Lubich C, Oseledets I, Vandereycken B, Verstraete F. Unifying time evolution and optimization with matrix product states. *Phys Rev B*. 2016;*94*(16):165116.
73. Haegeman J, Osborne TJ, Verstraete F. Post-matrix product state methods: to tangent space and beyond. *Phys. Rev. B*. 2013;*88*(7): 075133.
74. Cederbaum LS, Gindensperger E, Burghardt I. Short-time dynamics through conical intersections in macrosystems. *Phys Rev Lett*. 2005; *94*(11):113003.
75. Gindensperger E, Burghardt I, Lorenz S. Cederbaum. Short-time dynamics through conical intersections in macrosystems. II. Applications. *J Chem Phys*. 2006;*124*(14):144104.
76. Chin AW, Rivas Á, Huelga SF, Plenio MB. Exact mapping between system-reservoir quantum models and semi-infinite discrete chains using orthogonal polynomials. *J Math Phys*. 2010;*51*(9):092109.
77. Rams MM, Zwolak M. Breaking the entanglement barrier: tensor network simulation of quantum transport. *Phys Rev Lett*. 2020;*124* (13):137701.
78. Makri N. The linear response approximation and its lowest order corrections: an influence functional approach. *J Phys Chem B*. 1999; *103*(15):2823–9.
79. Tang Z, Ouyang X, Gong Z, Wang H, Jianlan W. Extended hierarchy equation of motion for the spin-boson model. *J Chem Phys*. 2015; *143*(22):224112.
80. Garg A, Onuchic JN, Ambegaokar V. Effect of friction on electron transfer in biomolecules. *J Chem Phys*. 1985;*83*(9):4491–503.
81. Maxim F, Gelin DE, Domcke W. Strong and long makes short: strong-pump strong-probe spectroscopy. *J Phys Chem Lett*. 2011;*2*(2): 114–9.
82. Moix J, Wu J, Huo P, Coker D, Cao J. Efficient energy transfer in light-harvesting systems, III: the influence of the eighth bacteriochlorophyll on the dynamics and efficiency in FMO. *J Phys Chem Lett*. 2011;*2*(24):3045–52.
83. Kreisbeck C, Kramer T. Long-lived electronic coherence in dissipative exciton dynamics of light-harvesting complexes. *J Phys Chem Lett*. 2012;*3*(19):2828–33.
84. Schulze J, Shibl MF, Al-Marri MJ, Kühn O. Multi-layer multi-configuration time-dependent Hartree (ML-MCTDH) approach to the correlated exciton-vibrational dynamics in the FMO complex. *J Chem Phys*. 2016;*144*(18):185101.
85. Schulze J, Kühn O. Explicit correlated exciton-vibrational dynamics of the FMO complex. *J Phys Chem B*. 2015;*119*(20):6211–6.
86. Wendling M, Pullerits T, Przyjalgowski MA, Vulto SIE, Aartsma TJ, van Grondelle R, et al. Electron-vibrational coupling in the Fenna-Matthews-Olson complex of Prosthecochloris aestuarii determined by temperature-dependent absorption and fluorescence line-narrowing measurements. *J Phys Chem B*. 2000;*104*(24):5825–31.
87. Ishizaki A, Fleming GR. Theoretical examination of quantum coherence in a photosynthetic system at physiological temperature. *PNAS*. 2009;*106*(41):17255–60.
88. Nalbach P, Braun D, Thorwart M. Exciton transfer dynamics and quantumness of energy transfer in the Fenna-Matthews-Olson complex. *Phys Rev E*. 2011;*84*(4):041926.
89. Chorošajev V, Rancova O, Abramavicius D. Polaronic effects at finite temperatures in the B850 ring of the LH2 complex. *Phys Chem Chem Phys*. 2016;*18*(11):7966–77.
90. Borrelli R, Thoss M, Wang H, Domcke W. Quantum dynamics of electron-transfer reactions: Photoinduced intermolecular electron transfer in a porphyrin–quinone complex. *Mol Phys*. 2012;*110*(9–10):751–63.
91. Borrelli R, Ellena S, Barolo C. Theoretical and experimental determination of the absorption and emission spectra of a prototypical indolenine-based squaraine dye. *Phys Chem Chem Phys*. 2014;*16*(6):2390–8.
92. Borrelli R, Peluso A. The vibrational progressions of the N→V electronic transition of ethylene: a test case for the computation of Franck-Condon factors of highly flexible photoexcited molecules. *J Chem Phys*. 2006;*125*(19):194308.
93. Borrelli R, Capobianco A, Peluso A. Franck–Condon factors—computational approaches and recent developments. *Can J Chem*. 2013; *91*(7):495–504.
94. Capobianco A, Borrelli R, Noce C, Peluso A. Franck–Condon factors in curvilinear coordinates: the photoelectron spectrum of ammonia. *Theor Chem Acc*. 2012;*131*(3):1181.
95. Reimers JR. A practical method for the use of curvilinear coordinates in calculations of normal-mode-projected displacements and Duschinsky rotation matrices for large molecules. *J Chem Phys*. 2001;*115*:9103–9.
96. Borrelli R, Peluso A. Quantum dynamics of radiationless electronic transitions including normal modes displacements and Duschinsky rotations: a second-order cumulant approach. *J Chem Theory Comput*. 2015;*11*(2):415–22.
97. Borrelli R, Peluso A. The temperature dependence of radiationless transition rates from ab initio computations. *Phys Chem Chem Phys*. 2011;*13*(10):4420.
98. Borrelli R, Domcke W. First-principles study of photoinduced electron-transfer dynamics in a mg–porphyrin–quinone complex. *Chem Phys Lett*. 2010;*498*:230–4.
99. Borrelli R, Capobianco A, Peluso A. Generating function approach to the calculation of spectral band shapes of free-base chlorin including Duschinsky and Herzberg-teller effects. *J Phys Chem A*. 2012;*116*(40):9934–40.
100. Tanimura Y, Kubo R. Two-time correlation functions of a system coupled to a heat Bath with a Gaussian-Markoffian interaction. *J Phys Soc Jpn*. 1989;*58*(4):1199–206.

101. Tanimura Y. Nonperturbative expansion method for a quantum system coupled to a harmonic-oscillator bath. *Phys Rev A*. 1990;*41*(12):6676–87.
102. Tanimura Y, Liouville S. Langevin, Fokker–Planck, and master equation approaches to quantum dissipative systems. *J Phys Soc Jpn*. 2006;*75*(8):082001.
103. Takahashi H, Tanimura Y. Open quantum dynamics theory of spin relaxation: application to μSR and low-field NMR spectroscopies. *J Phys Soc Jpn*. 2020;*89*(6):064710.
104. Tanaka M, Tanimura Y. Multistate electron transfer dynamics in the condensed phase: exact calculations from the reduced hierarchy equations of motion approach. *J Chem Phys*. 2010;*132*(21):214502.
105. Zhang J, Borrelli R, Tanimura Y. Proton tunneling in a two-dimensional potential energy surface with a non-linear system– bath interaction: thermal suppression of reaction rate. *J Chem Phys*. 2020;*152*(21):214114.
106. Kato A, Tanimura Y. Quantum heat current under non-perturbative and non-Markovian conditions: applications to heat machines. *J Chem Phys*. 2016;*145*(22):224105.
107. Kubo R. Generalized cumulant expansion method. *J Phys Soc Jpn*. 1962;*17*:1100.
108. Ishizaki A, Calhoun TR, Schlau-Cohen GS, Fleming GR. Quantum coherence and its interplay with protein environments in photosynthetic electronic energy transfer. *Phys Chem Chem Phys*. 2010;*12*(27):7319–37.
109. Jones FC, Birmingham TJ. When is quasi-linear theory exact? *Plasma Phys*. 1975;*17*(1):15.
110. Shi Q, Chen L, Nan G, Xu R-X, Yan YJ. Efficient hierarchical Liouville space propagator to quantum dissipative dynamics. *J Chem Phys*. 2009;*130*(8):084105.
111. Ishizaki A, Tanimura Y. Quantum dynamics of system strongly coupled to low-temperature colored noise bath: reduced hierarchy equations approach. *J Phys Soc Jpn*. 2005;*74*(12):3131–4.
112. Landi A, Borrelli R, Capobianco A, Velardo A, Peluso A. Second-order Cumulant approach for the evaluation of anisotropic hole mobility in organic semiconductors. *J Phys Chem C*. 2018;*122*(45):25849–57.
113. Gelin MF, Borrelli R, Domcke W. Origin of unexpectedly simple oscillatory responses in the excited-state dynamics of disordered molecular aggregates. *J Phys Chem Lett*. 2019;*10*(11):2806–10.
114. McLachlan AD. A variational solution of the time-dependent Schrodinger equation. *Mol Phys*. 1964;*8*(1):39–44.
115. Heller EJ. Time dependent variational approach to semiclassical dynamics. *J Chem Phys*. 1976;*64*(1):63–73.
116. Yan Y, Xing T, Shi Q. A new method to improve the numerical stability of the hierarchical equations of motion for discrete harmonic oscillator modes. *J Chem Phys*. 2020;*153*(20):204109.
117. Begušić T, Vaníček J. On-the-fly ab initio semiclassical evaluation of third-order response functions for two-dimensional electronic spectroscopy. *J Chem Phys*. 2020;*153*(18):184110.
118. Borrelli R, Gelin MF. Quantum dynamics of vibrational energy flow in oscillator chains driven by anharmonic interactions. *N J Phys*. 2020;*22*(12):123002.

How to cite this article: Borrelli R, Gelin MF. Finite temperature quantum dynamics of complex systems: Integrating thermo-field theories and tensor-train methods. *WIREs Comput Mol Sci*. 2021;e1539. https://doi.org/10.1002/wcms.1539